analytical chemistry

Article

Cite This: Anal. Chem. 2019, 91, 3951−3958

pubs.acs.org/ac

High Throughput Complementary Analysis and Quantitation of Metabolites by MALDI- and Silicon Nanopost Array-Laser Desorption/Ionization-Mass Spectrometry

Andrew R. Korte,*,† Nicholas J. Morris,‡ and Akos Vertes*,†

†Department of Chemistry, George Washington University, Washington, D.C. 20052, United States

‡UES, Inc., Dayton, Ohio 45432, United States

Supporting Information

ABSTRACT: Silicon nanopost array (NAPA) structures have been shown to be effective substrates for laser desorption/ionization-mass spectrometry (LDI-MS) and have been used to analyze a variety of samples including peptides, metabolites, drugs, explosives, and intact cells, as well as to image lipids and metabolites in tissue sections. However, no direct comparison has yet been conducted between NAPA-MS and the most commonly used LDI-MS technique, matrix-assisted laser desorption/ionization (MALDI)-MS. In this work, we compare the utility of NAPA-MS to that of MALDI-MS using two common matrices for the analysis of metabolites in cellular extracts and human urine. Considerable complementarity of molecular coverage was observed between the two techniques. Of 178 total metabolites assigned from cellular extracts, 68 were uniquely detected by NAPA-MS and 62 were uniquely detected by MALDI-MS. NAPA-MS was found to provide enhanced coverage of low-molecular weight compounds such as amino acids, whereas MALDI afforded better detection of larger, labile compounds including nucleotides. In the case of urine, a sample largely devoid of higher-mass labile compounds, 88 compounds were uniquely detected by NAPA-MS and 13 by MALDI-MS. NAPA-MS also favored more extensive alkali metal cation adduction relative to MALDI-MS, with the $[M + 2Na/K - H]^+$ species accounting for as much as 97% of the total metabolite ion signal in positive mode. The capability of NAPA-MS for targeted quantitation of endogenous metabolites in urine via addition of isotopically labeled standards was also examined. Both NAPA-MS and MALDI-MS provided quantitative results in good agreement with one another and the concentrations reported in the literature, as well as good sample-to-sample reproducibility (RSD < 10%).

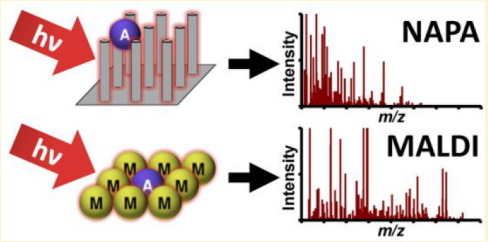

Metabolomics, the measurement of a broad range of metabolic products in a biological system, such as an organism or cell culture, allows for direct investigation of many observable phenomena such as disease, organismal/cellular variation, and response to stress. While these effects often have underlying genetic, epigenetic, or enzymatic causes, the systemic response at the cellular level (and by extension at the organismal level) is frequently dictated by the consequential small molecule perturbations. The existence and interrelation of multiple parallel pathways involving many metabolites, as well as the significant dependence on phenomena such as posttranslational modifications and enzymatic inhibition, mean that metabolic consequences cannot always be accurately predicted from genetic, transcriptomic, or proteomic analysis.[1] A complete understanding of the system and its underlying biochemistry, therefore, requires analysis of metabolic products themselves.[2]

Analytical techniques for the measurement of the complete or near-complete complement of human genes, transcripts, and proteins are well-established and widely available.[3−5] A number of challenges unique to metabolite analysis have precluded the establishment of a similar universal metabolomics technology. Unlike proteins and nucleic acids, which are composed of chemically similar monomer units, the catchall term "metabolites" includes a vast array of distinct chemical classes including gases, amino acids, nucleotides, vitamins and cofactors, lipids, xenobiotics, and many others. Moreover, metabolites span a vast range of concentrations within a typical cell. Rabinowitz et al., for example, reported intracellular metabolite concentrations spanning ∼5.5 orders of magnitude from iBMK cells.[6] The susceptibility of metabolites to alteration or degradation presents additional difficulties during sample preparation and analysis.[7]

In spite of these challenges, significant progress has been made in developing robust, widely applicable technologies for metabolomic analysis.[8−11] While several metabolomics studies have employed nuclear magnetic resonance for metabolite measurement,[12−14] mass spectrometry (MS) has emerged as the method of choice for metabolomics analysis.[2] Its inherent high sensitivity allows for the measurement of low-abundance metabolites, and the ability to perform accurate mass measurement and tandem MS for structural analysis allows for identification of detected compounds, a significant challenge in metabolomics due to the diversity of chemical species and the

Received: November 3, 2018
Accepted: February 20, 2019
Published: February 20, 2019

DOI: 10.1021/acs.analchem.8b05074
Anal. Chem. 2019, 91, 3951−3958

existence of multiple isomers and isobars.[15] Quantitation of metabolites by MS can be complicated by the wide range of metabolite ionization efficiencies and by matrix effects, but targeted quantitation is achievable if appropriate standards and methodologies are used.[6,16]

The typical MS metabolomics workflow uses either gas chromatography (GC) with electron ionization (EI) or liquid chromatography (LC) with electrospray ionization (ESI) for separation and ionization of analytes.[17] These techniques offer good quantitation and deep metabolome coverage, at the cost of lengthy analysis (typically in excess of 20 min per sample). Conversely, methods such as matrix-assisted laser desorption/ionization (MALDI) allow for shorter analysis times, with accompanying compromises in coverage.[18] For this reason, MALDI-MS has been applied for high-throughput metabolomics, where molecular depth of coverage is traded for reduced analysis times. The development of novel matrices and refinements in instrumentation have greatly expanded the capabilities of MALDI-MS analysis,[19] but the wide range of metabolite functionalities has hampered the development of a broad, untargeted MALDI-MS metabolomics approach. Experimental issues such as the formation of "hot spots"[20] and the effects of matrix−analyte ratio and salt concentration can complicate metabolite detection and quantitation.[21] Additionally, the use of small, organic matrices can lead to interference with or suppression of analyte signals.

A number of "matrix-free" laser desorption/ionization alternatives to MALDI have been developed, primarily utilizing inorganic materials to minimize interference and ion suppression. Such techniques include desorption/ionization on silicon (DIOS),[22] nanostructure initiator MS (NIMS),[23] and a wide array of techniques using nanoparticles,[24,25] nanowires,[26] and other nanoscale materials.[27]

Nanofabricated silicon nanopost array (NAPA) structures have previously been demonstrated as effective substrates for LDI-MS (herein called NAPA-MS).[28] Compared to other nanoscale LDI substrates, NAPA provides highly reproducible and controllable fabrication at the expense of increased production complexity and cost. Previous experiments have shown LDI-MS from NAPA to facilitate the detection of a broad range of compounds, with applications demonstrated for peptides,[28,29] explosives,[30] drugs,[31] metabolite extracts,[32] and tissue imaging.[33] The fundamentals of ion generation from nanopost arrays have been explored in some depth.[28,34,35] Briefly, coupling of parallel-polarized incident laser energy to nanoposts leads to absorption, local heating, and desorption/ionization of the deposited material. The roles of a number of critical parameters (including physical dimensions and optical and thermal properties) for NAPA and other nanostructure LDI methods have been discussed previously.[36] The mechanisms of desorption and ionization in MALDI have been extensively studied and debated, but it is now widely agreed that gas-phase interaction between desorbed matrix and analyte molecules plays a significant role in ion generation.[37−41]

The importance of this matrix−analyte interaction in MALDI and its inherent absence in matrix-free LDI techniques such as NAPA suggests that significant differences may exist in the capabilities of the two platforms to generate ions for MS analysis. Prior empirical comparison of MALDI with organic matrices and LDI with inorganic alternatives has shown preferential ionization of certain analytes using one method or the other.[42] In this work, we compare the high-throughput metabolomics capabilities of NAPA-MS and MALDI-MS in terms of metabolite coverage afforded, ionic species detected, and the ability to provide quantitative information from complex biological samples.

EXPERIMENTAL SECTION

Chemicals. Water (LC-MS grade; cat. no. W6), methanol (LC-MS grade; cat. no. A456), and chloroform (HPLC grade; cat. no. C607) were purchased from Fisher Scientific (Pittsburgh, PA). MALDI matrices (2,5-dihydroxybenzoic acid [DHB], ≥99.5%, cat. no. 39319; 9-aminoacridine [9-AA], ≥99.5%, cat. no. 92817) were purchased from Sigma-Aldrich (St. Louis, MO). Eagle's Minimum Essential Medium (EMEM, cat. no. 30-2003) was purchased from the American Type Culture Collection (ATCC; Manassas, VA). Methyl-d_3-creatine (97%, cat. no. DLM-1302) was purchased from Cambridge Isotope Laboratories (Tewksbury, MA). A reference urine sample (cat. no. 3672) was purchased from the US National Institute of Standards and Technology (Gaithersburg, MD), aliquoted upon receipt, and stored at −80 °C until use. NAPA fabrication details are available in the Supporting Information.

Cell Culture and Extraction. Immortalized human hepatocarcinoma cells (HepG2/C3A; ATCC, cat. no. CRL-10741) were cultured in EMEM medium under 5% CO_2 for 5 passages and then allowed to grow to confluence in 6 cm culture dishes. The medium was aspirated off, and the cells were quickly washed twice with 1 mL aliquots of 4 °C LC-MS grade water. Metabolism was quenched by the addition of 1 mL of 70% methanol at −80 °C, and the dishes were placed onto a dry ice bed for 5 min. The cells and quench solution were then scraped from the dish, transferred to 2 mL centrifuge tubes, placed on ice, and homogenized using an ultrasonic probe. To induce phase separation and remove interfering lipids and proteins, 1 mL of chloroform was added to each tube and the samples were vortexed for 1 min to mix thoroughly. The tubes were incubated for 30 min at −20 °C and then centrifuged at 13 000g and 4 °C for 10 min. The polar phases from the tubes were then pooled, aliquoted, dried in a vacuum centrifuge, and stored at −80 °C until use.

Sample Preparation and Deposition. Before use, hepatocyte extracts or urine aliquots were allowed to warm to room temperature. Hepatocyte extracts were reconstituted in 50 μL of LC-MS water and sonicated for 5 min. Urine was used as received from the provider. Both samples were serially diluted in water to provide dilution factors ranging from 1× (full concentration) to 3000×. Optimal dilution factors used for further experiments are presented in Table S-3. For NAPA-MS analysis, NAPA chips were affixed to a MALDI sample plate using double-sided tape and 500 nL of the sample was deposited onto each nanopost array and allowed to dry under atmosphere. For MALDI-MS analysis, DHB and 9-AA were separately dissolved at 10 mg/mL in methanol and mixed 1:1 with the metabolite extract or urine dilution, and 1 μL was deposited onto a stainless steel sample plate and allowed to dry under atmosphere. For quantitation experiments using isotopically labeled creatine, methyl-d_3-creatine in water was spiked into urine samples at a range of concentrations prior to dilution and analysis.

MS Analysis and Data Evaluation. Mass spectra were acquired using an LTQ Orbitrap XL mass spectrometer equipped with a MALDI source (Thermo Scientific, San Jose, CA). All MS spectra were acquired from m/z 100−1000 using the orbitrap analyzer at a resolving power setting of 30 000. For NAPA samples, the surface of each 2 mm diameter array was

DOI: 10.1021/acs.analchem.8b05074
Anal. Chem. 2019, 91, 3951−3958

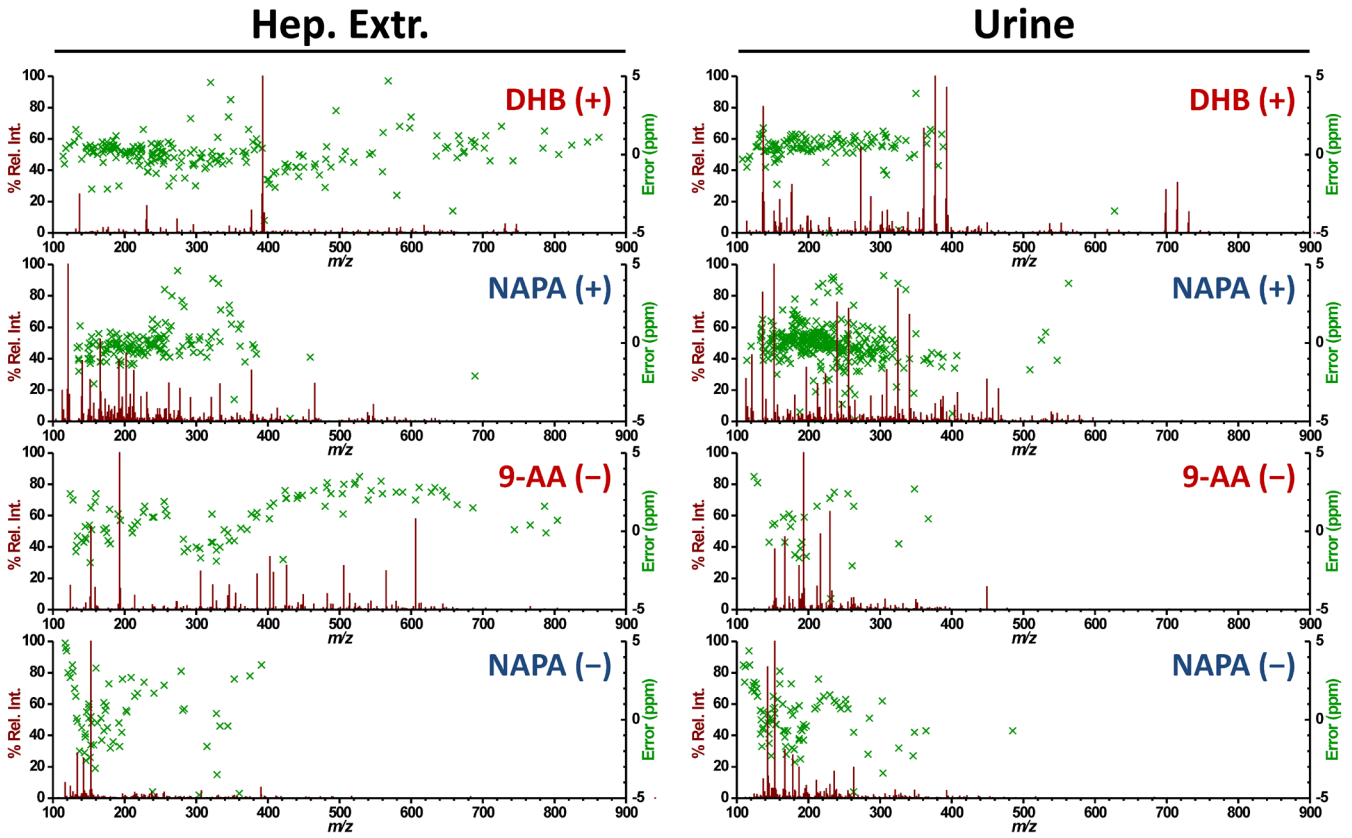

Figure 1. NAPA- and MALDI-MS spectra and assigned metabolite ion mass errors for hepatocyte extracts and urine. Spectra were obtained from optimal dilutions of all samples (see Table S-3).

interrogated using the tissue imaging function at a raster pitch setting of 100 μm with 1 scan per raster step and 10 laser shots per scan. The laser fluence used for NAPA experiments was ~32 mJ/cm^2. For MALDI samples, the crystal positioning system survey function was used to target areas of the sample well containing matrix/analyte crystals while minimizing the influence of matrix hot spots. Laser fluences for MALDI experiments were ~24 mJ/cm^2 for DHB and ~28 mJ/cm^2 for 9-AA. MALDI spectra were acquired in positive ion mode with DHB and negative ion mode with 9-AA, while NAPA spectra were acquired in both polarities from different sample spots. All analyses were conducted in triplicate or quadruplicate.

After acquisition, spectra were averaged and imported into mMass[43] for peak picking. For hepatocyte extracts, metabolite ions were assigned by matching m/z values of detected ions to theoretical m/z values for a compiled list of human metabolites and exogenous compounds (such as medium components) adapted from Roe et al.[44] and Psychogios et al.[45] (Table S-1). For urine samples, a list of metabolite ion masses was generated for compounds with a reported concentration of ≥1 μmol/mmol creatinine in the Urine Metabolome Database[46] (Table S-2). All ions were assigned with a m/z window of ±5 ppm. Spectra were deconvoluted by summing all detected species for a given compound ($[M + H]^+$, $[M + Na]^+$, etc.). Compounds for which cell extracts or urine yielded a summed intensity of at least ten times that in the corresponding blank were considered detected from the sample.

RESULTS AND DISCUSSION

Throughput and Metabolite Coverage. In this work, NAPA- and MALDI-MS acquisitions were accomplished in 2−7 min per sample. These short acquisition times, in conjunction with the inherent ability of LDI-based techniques to analyze multiple samples without the need for intersample equilibration, represent a significantly higher throughput than is obtained using most chromatographic metabolomics workflows. Moreover, subsequent analysis of acquired data suggested that acquisition times could be further shortened at a modest cost in molecular coverage. For example, interrogating an entire 2 mm diameter nanopost array in a positive ion NAPA-MS acquisition of a hepatocyte extract (~7 min acquisition time) yielded 90 assigned metabolites. Averaging a single raster pass across the sample (20 s acquisition time) yielded 64 assigned metabolites, demonstrating that even further improvements in throughput are possible at the further cost of depth of coverage.

Representative spectra and m/z errors for assigned metabolite ions are presented in Figure 1. S-1 and S-2 provide the number of detected compounds, after deconvolution of ionic species, for hepatocyte extract and urine dilutions, respectively. Figure 2 shows the overlap and complementarity of metabolite coverages afforded by the two techniques. A complete listing of assigned metabolites from hepatocyte extracts and urine is provided in Tables S-4 and S-5, respectively. As assignments are based on accurate m/z measurements alone, the presence of isomers and/or nearly isobaric ions cannot be excluded. Although a narrow m/z tolerance was used to minimize this effect to the degree possible, the complexity of biological samples prevents unambiguous assignment of many compounds. For example, an HMDB search of the ion detected at m/z 201.9335 with a ±5 ppm tolerance and allowing for the ionic species examined in this work yields only a single result ($[\text{taurine} + 2K - H]^+$). However, the ion detected at m/z 219.0263, herein assigned as

DOI: 10.1021/acs.analchem.8b05074
Anal. Chem. 2019, 91, 3951−3958

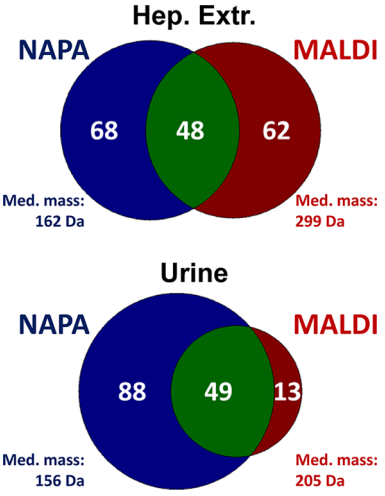

Figure 2. Numbers of metabolites assigned by accurate m/z in NAPA- and MALDI-MS analyses of hepatocyte extracts and urine samples at optimal dilution (see Table S-3). Median neutral masses for compounds uniquely detected by either technique are provided.

$[\text{glucose} + \text{K}]^+$, yields 40 possible assignments arising from three distinct molecular formulas, including many sugar and sugar alcohol isomers. HMDB IDs of assigned compounds are provided for reference but are not intended to exclude other potential assignments.

In the case of hepatocyte extracts, a high degree of complementarity was observed between NAPA- and MALDI-MS, with only 48 of the 178 total detected metabolites detected by both methods. Unique detection was afforded for 68 compounds by NAPA-MS and 62 compounds by MALDI-MS (Figure 2). Compounds detected using both techniques spanned a wide range of chemical functionalities and biological functions, including amino acids (e.g., glutamine and arginine), sugars and sugar phosphates (e.g., glucose and glucose phosphate), nitrogenous bases (e.g., adenine and guanine), and exogenous compounds from growth medium (e.g., penicillin G and phenol red indicator). Compounds detected only by MALDI-MS included a number of carnitine derivatives (carnitine, acetylcarnitine, propionylcarnitine, butyrylcarnitine, and valerylcarnitine) and nucleotides/nucleotide derivatives (e.g., adenosine mono-, di-, and triphosphate [AMP, ADP, and ATP], nicotinamide adenine dinucleotide [NAD], and flavin adenine dinucleotide [FAD]). Among the compounds uniquely detected by NAPA-MS were several amino acids (glycine, alanine, serine, proline, ornithine, lysine, methionine, asparagine, and phenylalanine) and a number of acetylated amino acids (acetylglycine, acetylcysteine, acetylornithine, acetylglutamine, acetylglutamic acid, and acetylhistidine). Due to an instrumental loss of sensitivity in spectra acquired over broad m/z ranges, the scanned range in these experiments was limited to m/z 100−1000. Six of the NAPA-specific compounds have neutral masses below the lower m/z boundary of the acquired spectra, and their unique detection by NAPA-MS may be attributed to its greater tendency to form alkali metal adduct species (see "Ionic Species Detected"). While it is unknown whether this benefit is applicable to other MALDI-MS systems, it does facilitate the detection of these low-mass compounds on the instrument used in this work.

From the urine samples, 49 metabolites were detected using both techniques, with 88 compounds uniquely detected by NAPA-MS and 13 by MALDI-MS. Both techniques provided detection of a range of compounds including well-known urinary constituents (creatinine, creatine, and phosphocreatine) as well as common xenobiotics and their metabolites (acetaminophen and its sulfate and glucuronide products, as well as ibuprofen). Similar to the hepatocyte extracts, a number of acylcarnitines (acetyl-, butyryl-, hydroxyvaleryl-, octanoyl-, and decanoylcarnitine) were detectable only by MALDI-MS, whereas detection of several amino acids (glycine, alanine, serine, asparagine, lysine, phenylalanine, tyrosine, and tryptophan) and acetylated amino acids (acetylornithine, acetylaspartic acid, acetylglutamine, and acetyllysine) was specific to NAPA-MS. Moreover, significant complementarity was observed between positive and negative ion mode acquisitions, emphasizing the need to acquire in both polarities to maximize metabolite coverage. Of the 178 total metabolites assigned from hepatocyte extracts across both NAPA- and MALDI-MS acquisitions, 114 were detected in only one polarity. From urine, 91 out of 150 total compounds were detected in only one polarity.

As can be seen from Figure 1, the m/z range of detected metabolites varies by technique and sample. In the analysis of hepatocyte extracts by NAPA in both polarities, a significant number of metabolite ions could be assigned below $m/z \sim 400$ but very few above this threshold. In contrast, MALDI using both DHB in positive ion mode and 9-AA in negative ion mode yielded assignable metabolite ions up to $m/z \sim 900$. The metabolites detected by MALDI between m/z 400 and 900 include a number of labile compounds such as nucleotides and nucleotide derivatives, which are highly sensitive to in-source fragmentation (ISF).[7] The extent of fragmentation of these species in MALDI-MS and the dependence on instrumental factors such as laser fluence have been previously investigated.[47] Prior NAPA-MS experiments have revealed the susceptibility of particularly labile species to ISF on this platform, especially at elevated laser fluence.[32,34] The detection here of nitrogenous nucleotide bases (adenine, etc.) by both techniques is, for example, believed to be primarily a result of ISF.

To evaluate the role of ISF in the apparent mass dependence of metabolite coverage by NAPA-MS relative to MALDI-MS, a standard of ATP was analyzed in negative ion mode by NAPA-MS and MALDI-MS using 9-AA as a matrix (Figure S-3). Even at the threshold fluence for ion generation by NAPA-MS (~8 mJ/cm^2), intact ATP was not detected. Increasing fluence was found to provide significant signal for ATP fragments (ADP, AMP, and adenine, as well as phosphate fragments), but the intact parent species was absent. A similar increase in fragmentation was observed with increasing fluence in MALDI-MS experiments, but at all tested fluences, the intact $[\text{ATP} - \text{H}]^-$ species was detectable. This increased ISF in NAPA-MS relative to MALDI-MS appears to be a significant reason for the complementarity observed between the two techniques. Past survival yield comparisons for LDI from silicon nanostructures and MALDI indicated higher internal energies for the ions produced by the former, which is consistent with the current observations.[34,48] Whereas small, mostly nonlabile compounds (e.g., amino acids) are detected more reliably by NAPA-MS, larger, more labile compounds are mostly or completely fragmented in the desorption/ionization process. This hypothesis is supported both by the identities of the MALDI-MS-specific compounds (especially nucleotides) and by an examination of the neutral masses of compounds specific to one technique or the other (median neutral mass ~162 Da for NAPA-MS compared to ~299 Da for MALDI-MS).

DOI: 10.1021/acs.analchem.8b05074
Anal. Chem. 2019, 91, 3951−3958

The loss of labile higher-MW compounds due to ISF is also supported by a comparison of the desorption mechanisms of NAPA and MALDI. Koubenakis et al. have reported peak surface temperatures of ∼1100 K for MALDI using DHB, with rapid cooling (<700 K within 30 ns) due primarily to evaporation of matrix molecules.[49] Similarly, Bae et al. reported plume temperatures of ∼800 K dropping to ∼400 K due to expansion of the MALDI plume.[50] Calculations for NAPA-LDI have yielded an estimated surface temperature of ∼1000 K for the post dimensions and fluence used in this work.[35] Given the similarity in peak temperatures for the two techniques, it is likely that the absence of a dense matrix-containing plume leads to slower dissipation of analyte internal energy and thus increased ISF. Prior work using NAPA precursors has indeed demonstrated increased internal energy for analytes desorbed from these structures relative to MALDI.[48]

Unlike for hepatocyte extracts, a limited degree of complementarity between NAPA- and MALDI-MS was observed for urine samples, presumably due to the lack of higher-mass labile compounds in urine compared to cellular extracts. The nucleotides and nucleotide derivatives detected exclusively or preferentially by MALDI-MS are present at very low levels in most urine samples.[46] Thus, for urine samples, NAPA-MS offers superior molecular coverage (137 metabolites) compared to MALDI-MS (62 metabolites). The urine data set was also investigated for potential relationships between (a) detected metabolite intensity and literature-reported metabolite concentration and (b) detected metabolite intensity and polarity (calculated octanol−water logP). Metabolite ion absolute intensity was observed to be weakly associated with metabolite abundance, likely due to the wide variability in ionization efficiencies across metabolite classes (Figure S-4). As expected for a urine sample, the detected species were predominantly polar in nature (median logP = −0.9), but a further dependence of signal intensity on polarity was not evident (Figure S-5).

Ionic Species Detected. Due to the mechanistic differences between NAPA- and MALDI-MS and the previously observed tendency of NAPA to generate otherwise uncommon alkali metal adducts (e.g., $[M + 2Na/K - H]^+$), the abundance of various adducts in both methods was compared. Figure 3 shows the percentage of total assigned metabolite intensity represented by the detected ionic species in positive ion mode. For both techniques, the assigned metabolite signal in positive ion mode is dominated by cation (Na^+ and K^+) adduct species. Both sample types (cell extract and urine) contain high concentrations of salts and provide plentiful Na^+ and K^+ ions for adduct formation, and the absence of separation from the analysis workflow leads to much greater degrees of cationization than are typically encountered in, for example, LC-MS-based metabolomics. Notably, appreciable signal (∼16% to ∼97% of assigned metabolite signal, depending on technique and sample) was also observed for species containing two alkali metal cations, in which a protic hydrogen is exchanged for Na^+ or K^+ in addition to adduction of another cation. Metabolite ions assigned from positive mode NAPA-MS were almost exclusively alkali metal adducts, with the $[M + Na]^+$, $[M + K]^+$, $[M + Na + K - H]^+$, $[M + 2Na - H]^+$, and $[M + 2K - H]^+$ species representing >99% of the total assigned signal intensity for both the cellular extract and urine. For MALDI-MS, these same species accounted for 72% of the signal from hepatocyte extracts and 66% of the signal from urine (Table S-6). In the case of MALDI-MS, matrix molecules provide a ready source of protons for the formation of $[M + H]^+$ species. In contrast, the silicon surface in NAPA-MS provides very few protons, and the overwhelming majority of detected species are sodium and potassium adducts. Differences in detected ionic species were far less pronounced in negative ion mode (Figure S-6), where ≥80% of the assigned metabolite signal consisted of either the $[M - H]^-$ or $[M - H - H2O]^-$ species (Table S-7).

In addition to the variability in adduct formation between NAPA- and MALDI-MS, a distinct variation was observed between sample types for both techniques. In the case of hepatocyte extracts, sodium-containing species ($[M + Na]^+$, $[M + 2Na - H]^+$, and $[M + Na + K - H]^+$) comprised ∼12% of the total assigned metabolite signal by NAPA-MS and ∼20% of that by MALDI-MS. In contrast, these species represented ∼57% and ∼43% of the assigned signal from NAPA- and MALDI-MS of urine samples, respectively. Conversely, potassium-containing species ($[M + K]^+$, $[M + 2K - H]^+$, and $[M + Na + K - H]^+$) comprised ∼97% and ∼65% of assigned NAPA- and MALDI-MS signal from hepatocytes and ∼73% and ∼29% of assigned signal from urine, respectively (Table 1). The differential abundance of sodium and potassium adducts is reflective of reported sodium−potassium ratios in cytosol ($Na^+/K^+ \approx 0.17-0.27$)[51] and urine ($Na^+/K^+ \approx 4.0$),[52] although the observed ion ratios are also complicated by factors such as affinity of metabolites for adduction of Na^+ and K^+ and fluence dependent changes in the relative alkali adduct abundances in LDI from silicon nanostructures.[35,53] Experiments with standards confirmed the dependence of detected ionic species on salt

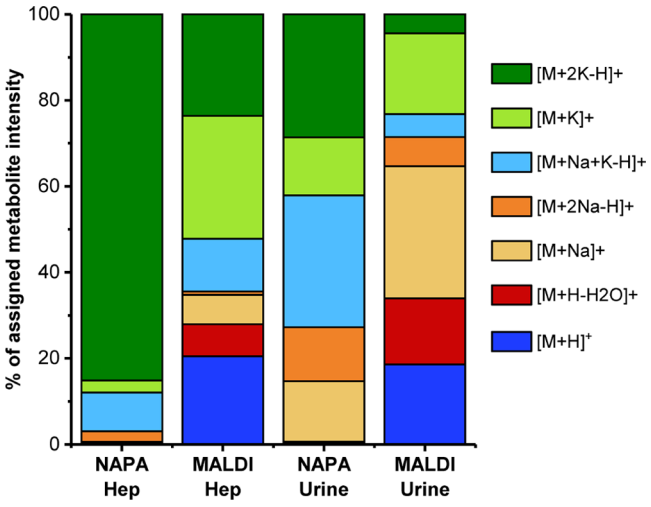

Figure 3. Ionic species distributions for assigned metabolite ions in positive ion mode NAPA- and MALDI-MS from optimal dilutions of hepatocyte extracts and urine.

Table 1. Percentage of Total Ion Intensity Represented by Na^+- and K^+-Containing Species in Positive Ion Mode NAPA- and MALDI-MS of Hepatocyte Extracts and Urine at Optimal Dilution Factor[a]

		Na^+ species, %	K^+ species, %
hep. extr.	NAPA	11.7	97.0
	MALDI	19.8	64.5
urine	NAPA	57.3	72.8
	MALDI	42.9	28.5

[a]Due to mixed adduction ($[M + Na + K - H]^+$ species), some values sum to >100.

DOI: 10.1021/acs.analchem.8b05074
Anal. Chem. 2019, 91, 3951−3958

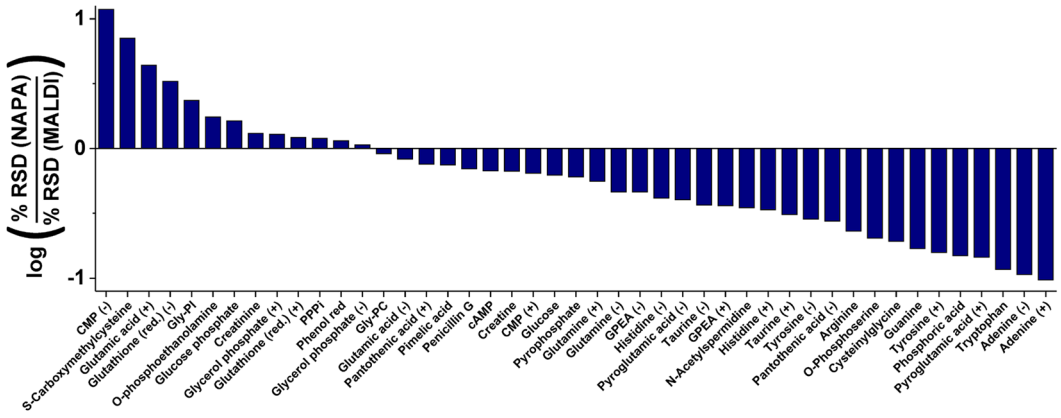

Figure 4. Comparison of absolute ion intensity %RSDs for 45 compounds detected in hepatocyte metabolite extracts by both NAPA- and MALDI-MS indicates lower %RSD in NAPA analyses for 32 species. Absolute intensities are obtained by summing signals for all assigned adduct species, and compounds detected in both polarities are presented separately and denoted (+) or (−). CMP: cytidine monophosphate. Gly-PI: glycerophosphoinositol. PPPi: inorganic triphosphate. Gly-PC: glycerophosphocholine. cAMP: cyclic adenosine monophosphate. GPEA: glycerophosphorylethanolamine.

concentration and suggested an improved tolerance of high salt concentrations for NAPA-MS compared to MALDI-MS. Acidification by addition of trifluoroacetic acid did not greatly affect signal for either NAPA- or MALDI-MS (Figure S-7).

Signal Reproducibility. To evaluate the variability of metabolite signals by MALDI- and NAPA-MS, compounds detected in hepatocyte extracts by both techniques were compared on the basis of the %RSD of absolute ion intensities across four analytical replicates (Figure 4). Of the 45 compounds detected in multiple samples by both methods, 32 exhibited a lower %RSD in NAPA analyses. Of the 13 compounds exhibiting lower variability in MALDI-MS experiments, most are of the labile bond-bearing type that are generally detected less strongly by NAPA-MS (e.g., phosphates). This result suggests that, in addition to offering greater coverage for smaller, robust metabolites, NAPA-MS also provides more reproducible signal for these compounds.

Creatine Quantitation in Urine. To compare the capabilities of NAPA- and MALDI-MS for quantitation of compounds of interest in a complex matrix, diluted urine samples were spiked with a range of concentrations of d_3-labeled creatine and analyzed by both techniques. The absolute ion intensities for creatine-d_3 were used to construct calibration curves (Figure 5), and the concentration of native (unlabeled) creatine was calculated using the native creatine absolute intensities and the calibration curves generated from the d_3-labeled standard. The measured concentration of creatine in undiluted urine was 166 ± 14 μM by NAPA-MS and 153 ± 15 μM by MALDI-MS. While urinary creatine levels can vary widely by individual and condition, these values are consistent with the range of urinary creatine concentrations provided in the human urine metabolome database (UMDB).[46] Absolute creatine ion intensities were not significantly affected by addition of creatine-d_3 for either technique. Additionally, NAPA- and MALDI-MS creatine measurements were in good agreement, yielding results within ~10% of one another, and both methods provided satisfactory analytical reproducibility, with %RSDs for both of <10%.

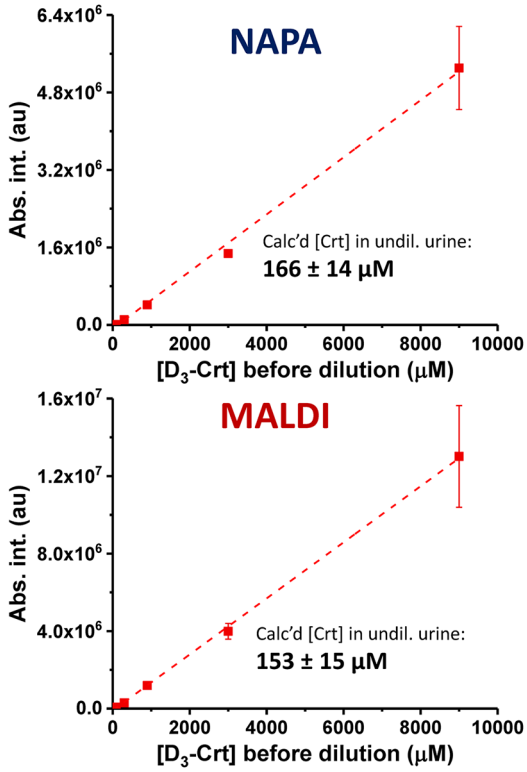

Figure 5. Absolute ion intensities of methyl-d_3-creatine in urine obtained by NAPA- and MALDI-MS.

CONCLUSIONS

Here, we have compared the capabilities of NAPA- and MALDI-MS for the high-throughput analysis of small molecule metabolites from biological samples. The highly complementary molecular coverage afforded by analysis of a cellular extract using the two techniques presents the possibility of using NAPA- and MALDI-MS in parallel to maximize the number of detected compounds, with NAPA-MS and MALDI-MS providing enhanced coverage for low-molecular weight, nonlabile compounds such as amino acids and for higher-molecular weight, labile compounds like nucleotides and their derivatives, respectively. Parallel utilization of these methods is facilitated by the very similar instrumentation requirements and workflows. In the case of samples lacking in higher-molecular weight metabolites (such as the urine tested here), NAPA-MS may

DOI: 10.1021/acs.analchem.8b05074
Anal. Chem. 2019, 91, 3951−3958

provide improved molecular coverage compared to MALDI-MS. It should be noted, however, that here we have limited the comparison of NAPA-MS to two of the most commonly used MALDI matrices (DHB and 9-AA). Since the choice of matrix can significantly impact the compounds detected from a given sample, additional comparisons to alternative matrices would be valuable. The comparable performance of NAPA-MS relative to MALDI-MS demonstrates its utility for rapid quantitation of targeted analytes even in a complex matrix and suggests possible screening or diagnostic applications.

■ ASSOCIATED CONTENT

Supporting Information

The Supporting Information is available free of charge on the ACS Publications website at DOI: 10.1021/acs.analchem.8b05074.

Procedure for NAPA fabrication and salt/TFA addition experiments; results of hepatocyte extract and urine dilution experiments; fluence dependence of NAPA- and MALDI-MS spectra from an ATP standard; comparisons of metabolite intensities to reported abundance and polarity for NAPA- and MALDI-MS analysis of urine samples; tables of compounds used to generate theoretical m/z values for metabolite assignment; tables of detected compounds in hepatocyte and urine extracts; tables of ionic species distributions for NAPA- and MALDI-MS analysis of hepatocyte extracts and urine (PDF)

■ AUTHOR INFORMATION

Corresponding Authors

*E-mail: vertes@gwu.edu. Phone: +1 202-994-2717. Fax: +1 202-994-5873.

*E-mail: korte@gwu.edu. Phone: +1 202-994-2332. Fax: +1 202-994-5873.

ORCID

Andrew R. Korte: 0000-0003-4270-966X

Akos Vertes: 0000-0001-5186-5352

Notes

The authors declare no competing financial interest.

■ ACKNOWLEDGMENTS

Research was sponsored by the U.S. Army Research Office and the Defense Advanced Research Projects Agency and was accomplished under Cooperative Agreement Number W911NF-14-2-0020. The views and conclusions contained in this document are those of the authors and should not be interpreted as representing the official policies, either expressed or implied, of the Army Research Office, DARPA, or the U.S. Government. The authors gratefully acknowledge the University of California, Santa Barbara Nanofabrication Facility for production of the nanopost arrays used in this work. The authors also acknowledge the work of Ms. Lida Parvin in culturing and providing the HepG2/C3A cells used here.

■ REFERENCES

(1) Carrari, F.; Baxter, C.; Usadel, B.; Urbanczyk-Wochniak, E.; Zanor, M.-I.; Nunes-Nesi, A.; Nikiforova, V.; Centero, D.; Ratzka, A.; Pauly, M.; Sweetlove, L. J.; Fernie, A. R. *Plant Physiol.* **2006**, *142*, 1380−1396.

(2) Johnson, C. H.; Ivanisevic, J.; Siuzdak, G. *Nat. Rev. Mol. Cell Biol.* **2016**, *17*, 451−459.

(3) Shendure, J.; Ji, H. *Nat. Biotechnol.* **2008**, *26*, 1135−1145.

(4) Wang, Z.; Gerstein, M.; Snyder, M. *Nat. Rev. Genet.* **2009**, *10*, 57−63.

(5) Vidova, V.; Spacil, Z. *Anal. Chim. Acta* **2017**, *964*, 7−23.

(6) Park, J. O.; Rubin, S. A.; Xu, Y.-F.; Amador-Noguez, D.; Fan, J.; Shlomi, T.; Rabinowitz, J. D. *Nat. Chem. Biol.* **2016**, *12*, 482.

(7) Xu, Y.-F.; Lu, W.; Rabinowitz, J. D. *Anal. Chem.* **2015**, *87*, 2273−2281.

(8) Zhang, A.; Sun, H.; Wang, P.; Han, Y.; Wang, X. *Analyst* **2012**, *137*, 293−300.

(9) Newgard, C. B. *Cell Metab.* **2017**, *25*, 43−56.

(10) Markley, J. L.; Bruschweiler, R.; Edison, A. S.; Eghbalnia, H. R.; Powers, R.; Raftery, D.; Wishart, D. S. *Curr. Opin. Biotechnol.* **2017**, *43*, 34−40.

(11) Allard, P. M.; Genta-Jouve, G.; Wolfender, J. L. *Curr. Opin. Chem. Biol.* **2017**, *36*, 40−49.

(12) Kim, H. K.; Choi, Y. H.; Verpoorte, R. *Nat. Protoc.* **2010**, *5*, 536−549.

(13) Emwas, A.-H. M.; Salek, R. M.; Griffin, J. L.; Merzaban, J. *Metabolomics* **2013**, *9*, 1048−1072.

(14) Nagana Gowda, G. A.; Raftery, D. *Anal. Chem.* **2017**, *89*, 490−510.

(15) Dias, D.; Jones, O.; Beale, D.; Boughton, B.; Benheim, D.; Kouremenos, K.; Wolfender, J.-L.; Wishart, D. *Metabolites* **2016**, *6*, 46.

(16) Wu, Y.; Li, L. *J. Chromatogr. A* **2016**, *1430*, 80−95.

(17) Cajka, T.; Fiehn, O. *Anal. Chem.* **2016**, *88*, 524−545.

(18) Nordström, A.; Want, E.; Northen, T.; Lehtiö, J.; Siuzdak, G. *Anal. Chem.* **2008**, *80*, 421−429.

(19) Dreisewerd, K. *Anal. Bioanal. Chem.* **2014**, *406*, 2261−2278.

(20) Luxembourg, S. L.; McDonnell, L. A.; Duursma, M. C.; Guo, X.; Heeren, R. M. *Anal. Chem.* **2003**, *75*, 2333−2341.

(21) Shroff, R.; Rulíšek, L.; Doubský, J.; Svatoš, A. *Proc. Natl. Acad. Sci. U. S. A.* **2009**, *106*, 10092−10096.

(22) Thomas, J. J.; Shen, Z.; Crowell, J. E.; Finn, M. G.; Siuzdak, G. *Proc. Natl. Acad. Sci. U. S. A.* **2001**, *98*, 4932−4937.

(23) Northen, T. R.; Yanes, O.; Northen, M. T.; Marrinucci, D.; Uritboonthai, W.; Apon, J.; Golledge, S. L.; Nordström, A.; Siuzdak, G. *Nature* **2007**, *449*, 1033−1036.

(24) Wen, X.; Dagan, S.; Wysocki, V. H. *Anal. Chem.* **2007**, *79*, 434−444.

(25) Chu, H. W.; Unnikrishnan, B.; Anand, A.; Mao, J. Y.; Huang, C. C. *J. Food Drug Anal.* **2018**, *26*, 1215−1228.

(26) Go, E. P.; Apon, J. V.; Luo, G.; Saghatelian, A.; Daniels, R. H.; Sahi, V.; Dubrow, R.; Cravatt, B. F.; Vertes, A.; Siuzdak, G. *Anal. Chem.* **2005**, *77*, 1641−1646.

(27) Lu, M.; Yang, X.; Yang, Y.; Qin, P.; Wu, X.; Cai, Z. *Nanomaterials* **2017**, *7*, 87.

(28) Walker, B. N.; Stolee, J. A.; Pickel, D. L.; Retterer, S. T.; Vertes, A. *J. Phys. Chem. C* **2010**, *114*, 4835−4840.

(29) Stopka, S. A.; Holmes, X. A.; Korte, A. R.; Compton, L. R.; Retterer, S. T.; Vertes, A. *Adv. Funct. Mater.* **2018**, *28*, 1801730.

(30) Walker, B. N.; Stolee, J. A.; Vertes, A. *Anal. Chem.* **2012**, *84*, 7756−7762.

(31) Morris, N. J.; Anderson, H.; Thibeault, B.; Vertes, A.; Powell, M. J.; Razunguzwa, T. T. *RSC Adv.* **2015**, *5*, 72051−72057.

(32) Korte, A. R.; Stopka, S. A.; Morris, N.; Razunguzwa, T.; Vertes, A. *Anal. Chem.* **2016**, *88*, 8989−8996.

(33) Stopka, S. A.; Rong, C.; Korte, A. R.; Yadavilli, S.; Nazarian, J.; Razunguzwa, T. T.; Morris, N. J.; Vertes, A. *Angew. Chem., Int. Ed.* **2016**, *55*, 4482−4486.

(34) Stolee, J. A.; Vertes, A. *Phys. Chem. Chem. Phys.* **2011**, *13*, 9140−9146.

(35) Walker, B. N.; Stolee, J. A.; Pickel, D. L.; Retterer, S. T.; Vertes, A. *Appl. Phys. A: Mater. Sci. Process.* **2010**, *101*, 539−544.

(36) Stolee, J. A.; Walker, B. N.; Zorba, V.; Russo, R. E.; Vertes, A. *Phys. Chem. Chem. Phys.* **2012**, *14*, 8453−8471.

(37) Dreisewerd, K. *Chem. Rev.* **2003**, *103*, 395−426.

(38) Knochenmuss, R.; Zenobi, R. *Chem. Rev.* **2003**, *103*, 441−452.

(39) Karas, M.; Kruger, R. *Chem. Rev.* **2003**, *103*, 427−440.

(40) Knochenmuss, R. *Analyst* **2006**, *131*, 966−986.

DOI: 10.1021/acs.analchem.8b05074
Anal. Chem. 2019, 91, 3951−3958

(41) Jaskolla, T. W.; Karas, M. *J. Am. Soc. Mass Spectrom.* **2011**, *22*, 976−988.
(42) Yagnik, G. B.; Hansen, R. L.; Korte, A. R.; Reichert, M. D.; Vela, J.; Lee, Y. J. *Anal. Chem.* **2016**, *88*, 8926−8930.
(43) Strohalm, M.; Kavan, D.; Novák, P.; Volný, M.; Havlíček, V. *Anal. Chem.* **2010**, *82*, 4648−4651.
(44) Roe, B.; Kensicki, E.; Mohney, R.; Hall, W. W. *PLoS One* **2011**, *6*, e23641.
(45) Psychogios, N.; Hau, D. D.; Peng, J.; Guo, A. C.; Mandal, R.; Bouatra, S.; Sinelnikov, I.; Krishnamurthy, R.; Eisner, R.; Gautam, B.; Young, N.; Xia, J.; Knox, C.; Dong, E.; Huang, P.; Hollander, Z.; Pedersen, T. L.; Smith, S. R.; Bamforth, F.; Greiner, R.; et al. *PLoS One* **2011**, *6*, e16957.
(46) Bouatra, S.; Aziat, F.; Mandal, R.; Guo, A. C.; Wilson, M. R.; Knox, C.; Bjorndahl, T. C.; Krishnamurthy, R.; Saleem, F.; Liu, P.; Dame, Z. T.; Poelzer, J.; Huynh, J.; Yallou, F. S.; Psychogios, N.; Dong, E.; Bogumil, R.; Roehring, C.; Wishart, D. S. *PLoS One* **2013**, *8*, e73076.
(47) Steinhoff, R. F.; Krismer, J.; Eyer, K.; Fagerer, S. R.; Ibanez, A.; Pabst, M.; Zenobi, R. *Anal. Biochem.* **2014**, *447*, 107−113.
(48) Stolee, J. A.; Chen, Y.; Vertes, A. *J. Phys. Chem. C* **2010**, *114*, 5574−5581.
(49) Koubenakis, A.; Frankevich, V.; Zhang, J.; Zenobi, R. *J. Phys. Chem. A* **2004**, *108*, 2405−2410.
(50) Bae, Y. J.; Moon, J. H.; Kim, M. S. *J. Am. Soc. Mass Spectrom.* **2011**, *22*, 1070−1078.
(51) Page, M. J.; Di Cera, E. *Physiol. Rev.* **2006**, *86*, 1049−1092.
(52) O'Donnell, M.; Mente, A.; Rangarajan, S.; McQueen, M. J.; Wang, X.; Liu, L.; Yan, H.; Lee, S. F.; Mony, P.; Devanath, A.; Rosengren, A.; Lopez-Jaramillo, P.; Diaz, R.; Avezum, A.; Lanas, F.; Yusoff, K.; Iqbal, R.; Ilow, R.; Mohammadifard, N.; Gulec, S.; et al. *N. Engl. J. Med.* **2014**, *371*, 612−623.
(53) Chen, Y.; Vertes, A. *Anal. Chem.* **2006**, *78*, 5835−5844.

DOI: 10.1021/acs.analchem.8b05074
Anal. Chem. 2019, 91, 3951−3958

Supporting Information

High Throughput Complementary Analysis and Quantitation of Metabolites by MALDI- and Silicon Nanopost Array-Laser Desorption Ionization Mass Spectrometry

Andrew R. Korte[†]*, Nicholas Morris[‡], and Akos Vertes[†]*

[†]Department of Chemistry, George Washington University, Washington, DC 20052, USA
[‡] UES, Inc., Dayton, OH 45432, USA

Corresponding Authors:
*Email: vertes@gwu.edu, Phone: +1 202-994-2717, Fax: +1 202-994-5873
*Email: korte@gwu.edu, Phone: +1 202-994-2332, Fax: +1 202-994-5873

ORCID
Andrew R. Korte: 0000-0003-4270-966X

Nicholas J. Morris: 0000-0001-7233-4032
Akos Vertes: 0000-0001-5186-5352

TABLE OF CONTENTS

Fabrication of Nanopost Arrays. NAPA were produced from low resistivity p-type silicon wafers (0.005-0.1 Ω·cm) purchased from Silicon Valley Microelectronics, Inc. (Santa Clara, CA). Wafers were spin coated with DUV 42P anti-reflective coating from Brewer Science (Rolla, MO) at 3500 RPM for 30 s, followed by a bake at 220 °C for 60 s. A 2:1 mixture of UVN-30 negative photoresist from Rohm and Haas Electronic Materials (Marlborough, MA) and AZ edge bead remover from AZ Electronic Materials (Somerville, NJ) was then spin coated at 2000 RPM for 40 s. A pre-exposure bake was performed on a 110 °C hotplate for 90 s. Photopatterning was performed using a 5500/300 248 nm deep-UV projection photolithography stepper from ASML (Veldhoven, AN) with an exposure energy of 104 mJ. A post-exposure bake was performed at 105 °C for 65 s on hot plate. The pattern was developed in 300MIF from AZ Electronic Materials (Somerville, NJ) developer for 20 s, rinsed with DI water for 40 s, and dried with nitrogen gas at 20 psi.

Etching was performed using a Plasma-Therm 770 SLR Fluorine ICP deep reactive-ion etching system (St. Petersburg, FL). The anti-reflective coating was etched for 30 s at 20 sccm of O2, 10 mTorr pressure, and an RF power of 100 W. Silicon etching was performed in a single etch step with the following gas parameters and powers: C4F8 = 17 sccm, SF6 = 10 sccm, CF4 = 9 sccm, 20 mTorr pressure, RF power = 18 W, ICP power = 825 W, with backside He cooling at a pressure of 7 Torr.

Plasma cleaning was performed post-etch using a Technics PEII oxygen plasma asher (Pleasanton, CA) at 300 mTorr and 100 W for 120 s. Further cleaning was achieved with a Nanostrip from Cyantek (Fremont, CA) bath at 70 °C for 10 min, followed by a rinse in DI water, and drying with nitrogen gas.

Analysis of Standards with Salt/TFA Addition. Sodium chloride (NaCl; cat. no. S3014), potassium chloride (KCl; cat. no. P9333), and trifuloroacetic acid (TFA; cat. no. T6508) were purchased from Sigma-Aldrich (St. Louis, MO). An equimolar mixture of glutamine, arginine, glucose, and tryptophan was prepared by dissolving each in water and mixing to yield a final concentration of each standard of 250 µM. NaCl, KCl, and TFA were each dissolved/diluted in water and then serially diluted and added to aliquots of the standard mixture to yield concentrations ranging from 5 µM to 50 mM (NaCl and KCl) or 0.001% to 1% (TFA). For NAPA-MS, 500 nL was pipetted directly onto NAPA and allowed to dry under atmosphere. For MALDI-MS, sample solutions were mixed 1:1 with matrix (DHB) in methanol (10 mg/mL) and 1 µL was spotted onto a stainless steel sample plate. All samples were analyzed as described in the main text.

Optimal Sample Dilutions. As expected, serial dilution of both hepatocyte extracts and urine showed the number of detectable metabolites to be highly dependent upon the concentration of the sample. Supplemental Figures S-1 and S-2 show the number of compounds detected at a range of dilution factors for hepatocyte extracts and urine, respectively. At high concentrations, poor signal was obtained from hepatocyte extracts using DHB and from urine using both DHB and 9-AA, likely owing to poor crystallization caused by high salt concentration. For NAPA-MS analysis, the number of detected compounds was highest at or near the highest concentration, although some signal loss was observed with undiluted urine samples, probably as a result of optical insulation of the posts by deposited material. Based on these results, further comparison was conducted using the undiluted samples for NAPA-MS of hepatocyte extracts, 3×-diluted samples for NAPA-MS of urine, undiluted samples for MALDI-MS using 9-AA of hepatocyte extracts, 10×-diluted samples for MALDI-MS using 9-AA of urine, and 30×-diluted samples for MALDI-MS using DHB of both hepatocyte extracts and urine (Table 1).

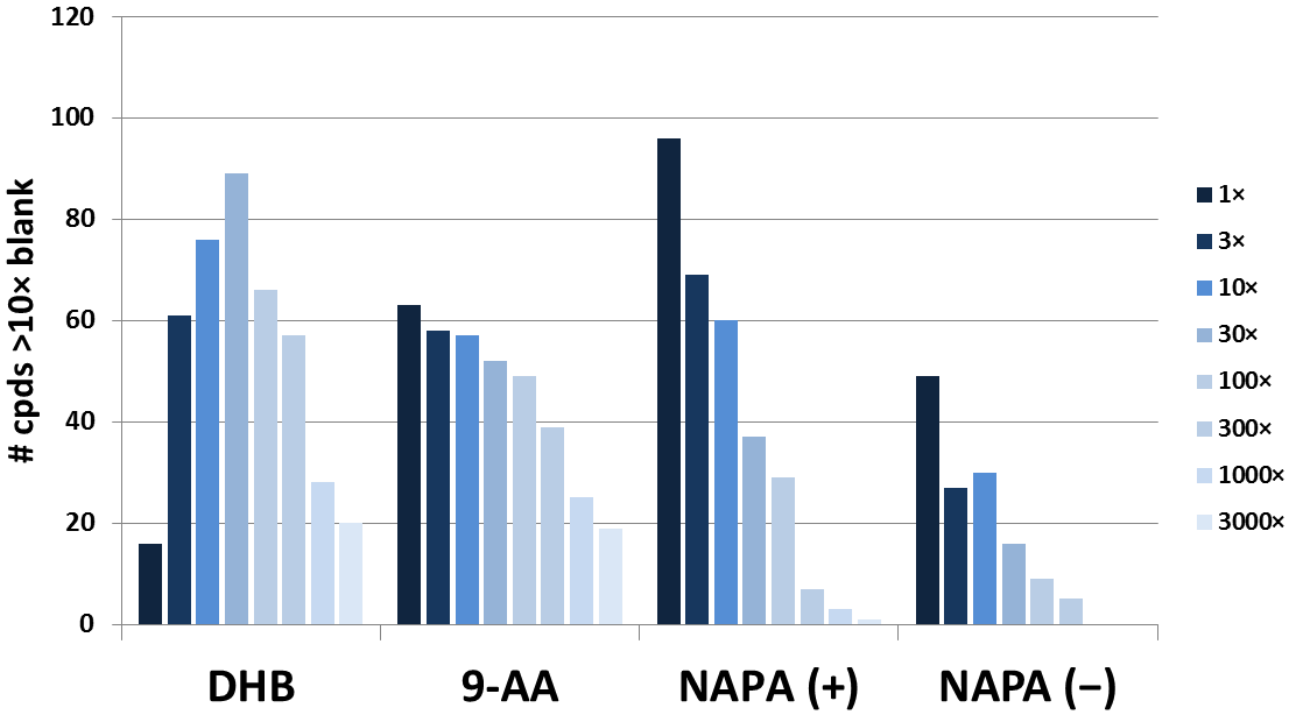

Figure S-1. Number of metabolites assigned by accurate *m/z* measurements from hepatocyte extract dilutions. Numbers include only compounds with summed absolute intensity >10× relative to blank.

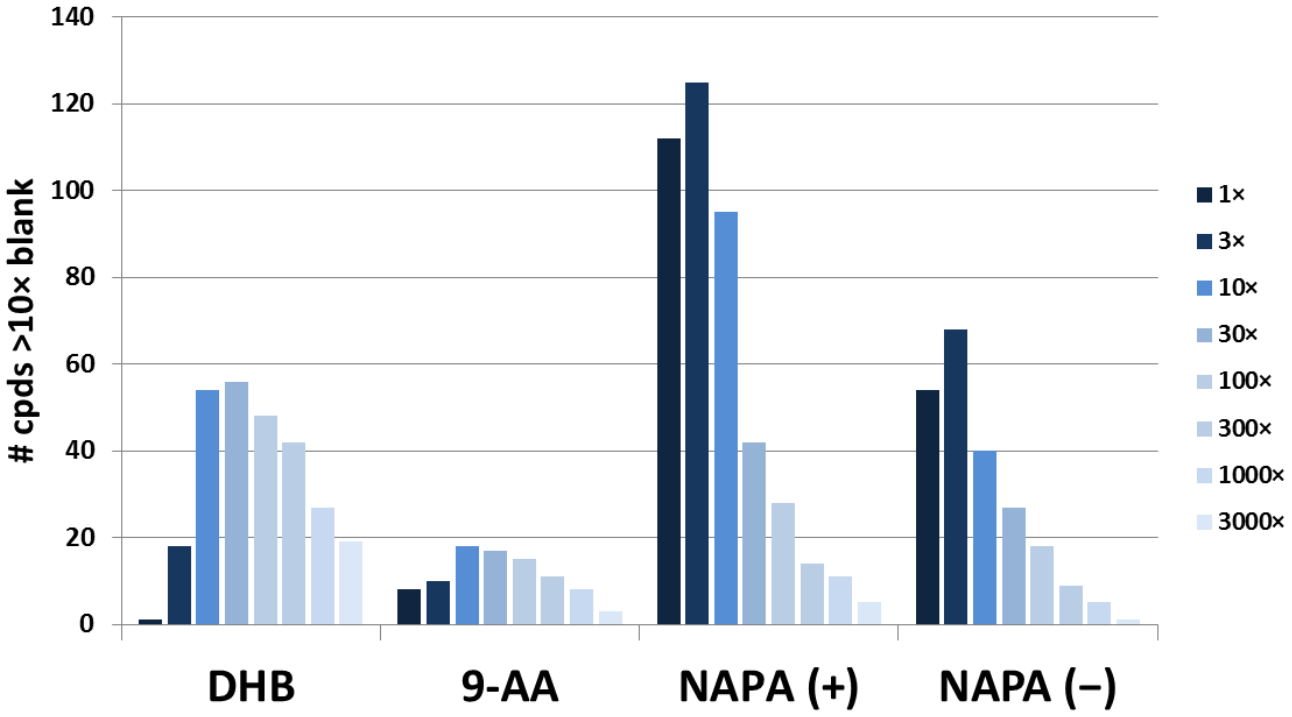

Figure S-2. Number of metabolites assigned by accurate *m/z* measurements from urine dilutions. Numbers include only compounds with summed absolute intensity >10× relative to blank.

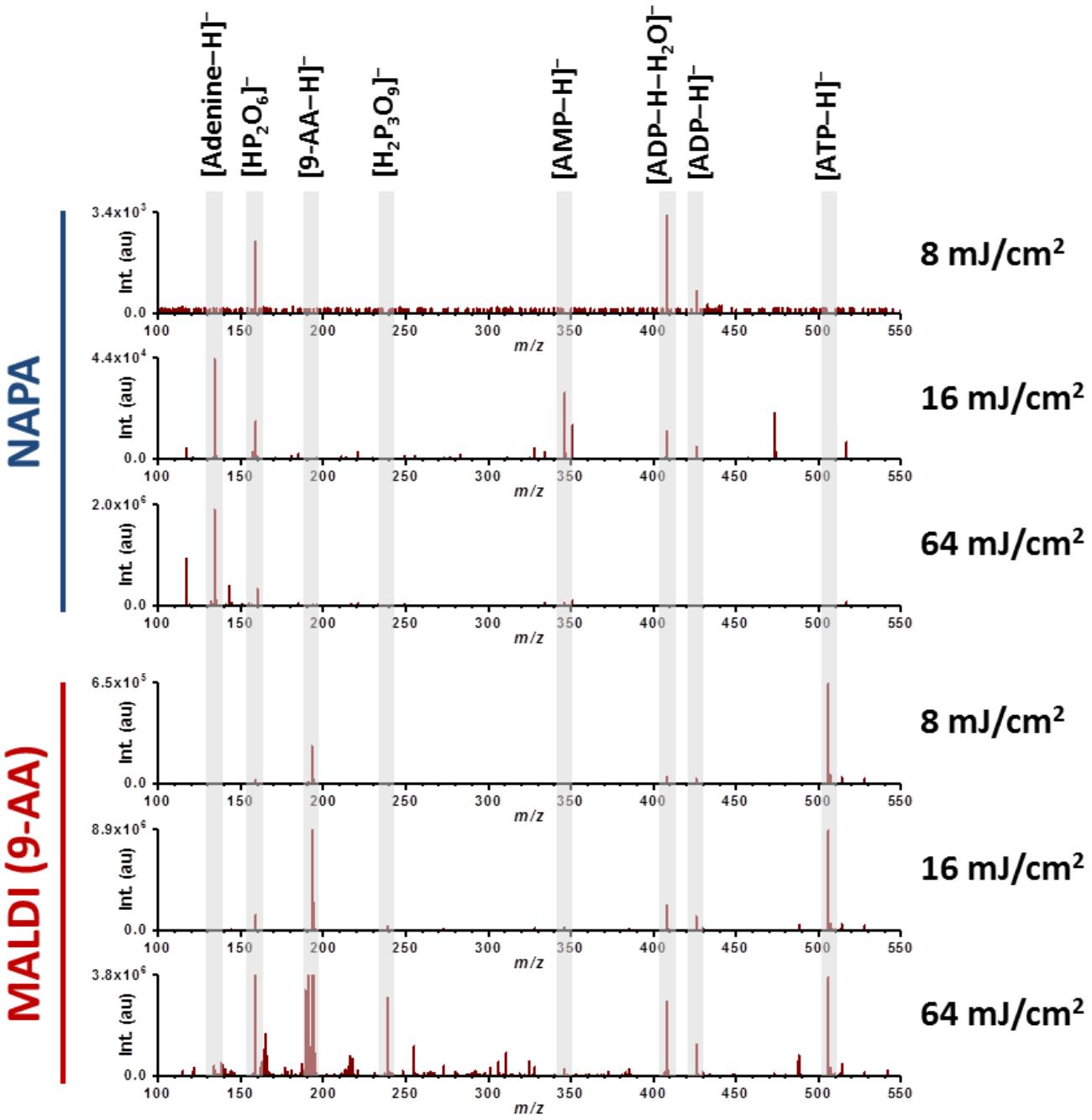

Figure S-3. NAPA- and MALDI-MS spectra of adenosine triphosphate (ATP) standard at varied laser fluence. Spectra are normalized to the highest-intensity assigned analyte peak.

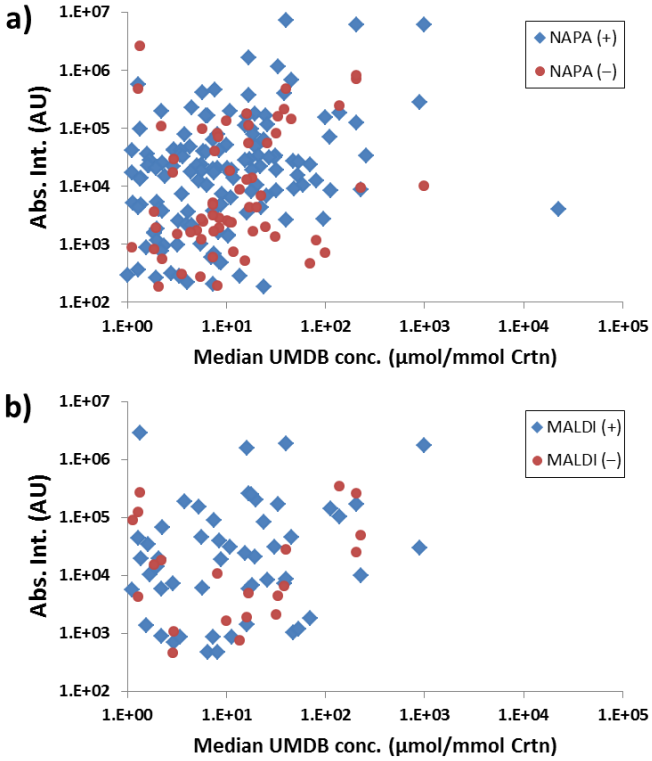

Figure S-4. Absolute NAPA- (a) and MALDI-MS (b) intensities for metabolite ions in urine samples vs. median reported concentration in the UMDB database.

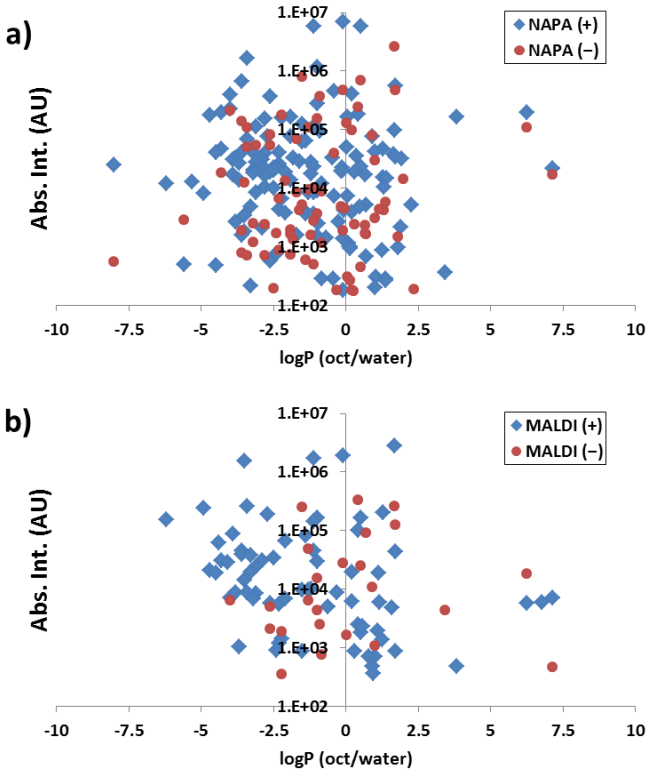

Figure S-5. Absolute NAPA- (a) and MALDI-MS (b) intensities for metabolite ions in urine samples vs. calculated octanol/water partitioning coefficients obtained from the UMDB database.

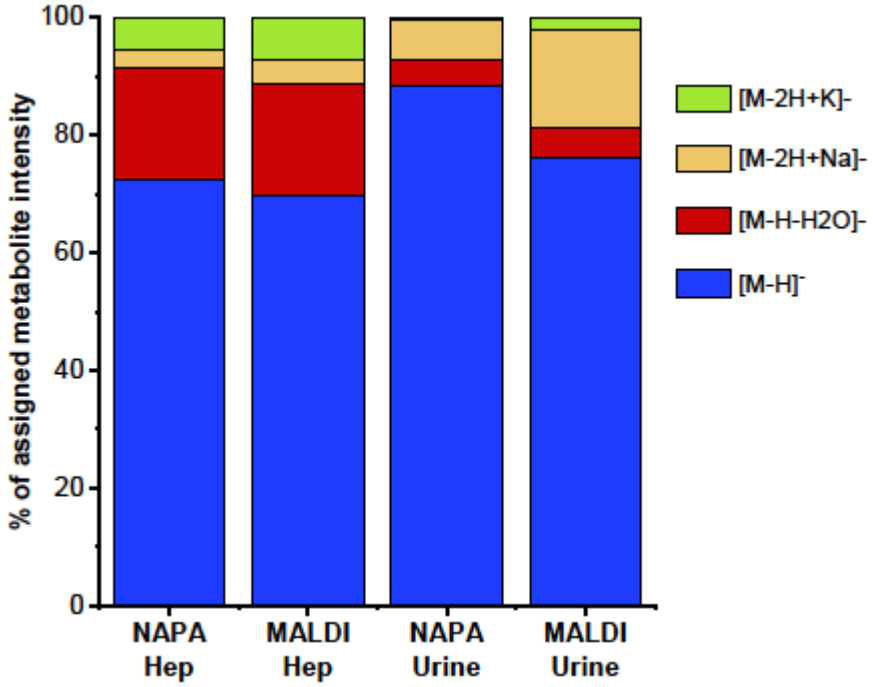

Figure S-6. Ionic species distributions for assigned metabolite ions in negative ion mode NAPA- and MALDI-MS from optimal dilutions of hepatocyte extracts and urine.

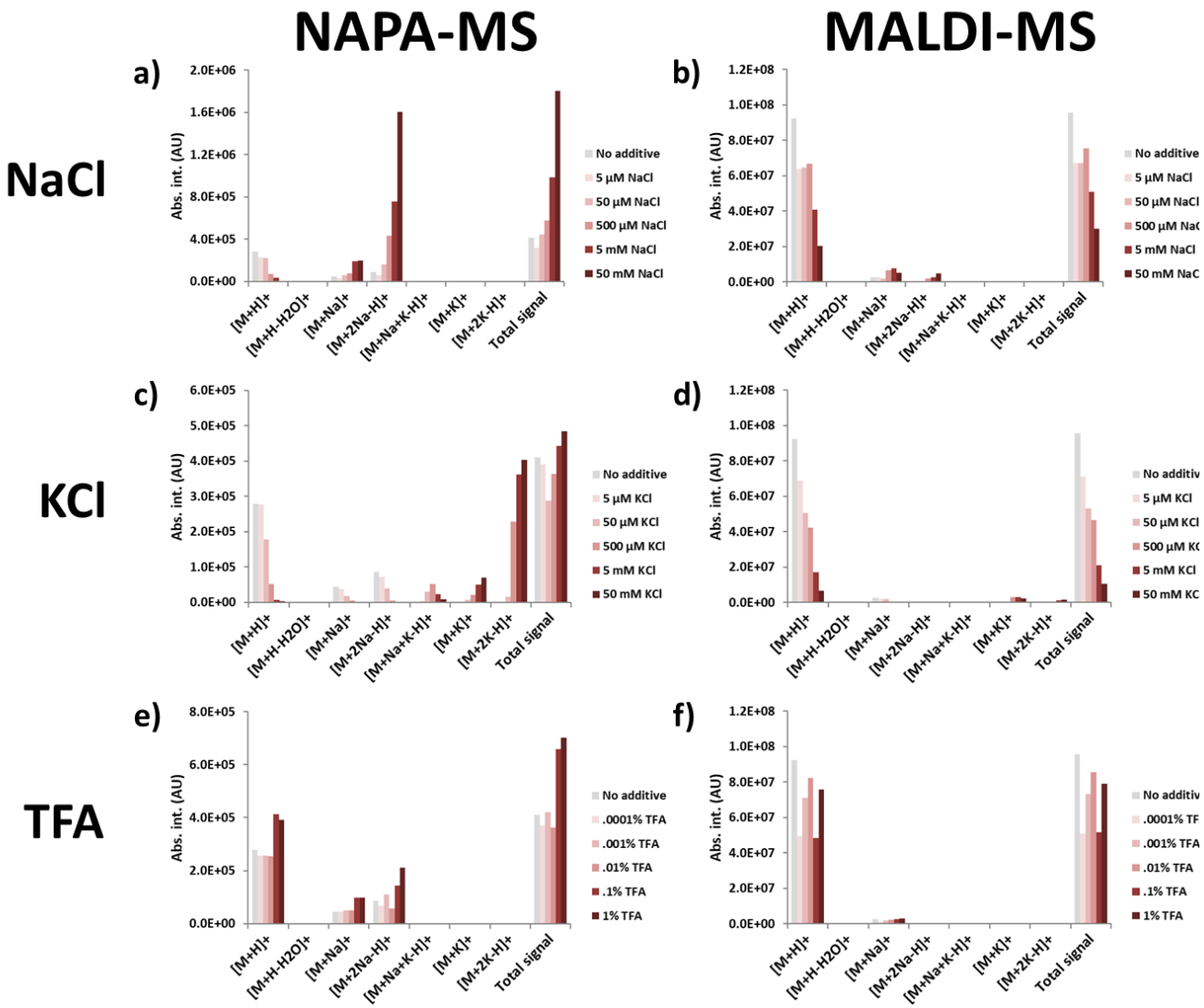

Figure S-7. Absolute intensities for several ionic species obtained from NAPA- and MALDI-MS analysis of a mixture of metabolite standards (glutamine, arginine, glucose, and tryptophan) at a range of additive (NaCl [a,b]; KCl [c,d]; trifluoroacetic acid [e,f]) concentrations.

Table S-1. Compiled list of endogenous human metabolites and exogenous compounds used to assign metabolite ions in hepatocyte extracts.

HMDB ID	Name	Formula	Neutral mass (Da)
HMDB0003338	Hydroxylamine	H3NO	33.0215
HMDB0000142	Formic acid	CH2O2	46.0055
HMDB0000042	Acetic acid	C2H4O2	60.0211
HMDB0000294	Urea	CH4N2O	60.0324
HMDB0000149	Ethanolamine	C2H7NO	61.0528
HMDB0006112	Malondialdehyde	C3H4O2	72.0211
HMDB0000123	Glycine	C2H5NO2	75.0320
HMDB0001881	Propylene glycol	C3H8O2	76.0524
HMDB0002991	Cysteamine	C2H7NS	77.0299
HMDB0000243	Pyruvic acid	C3H4O3	88.0160
HMDB0001873	Isobutyric acid	C4H8O2	88.0524
HMDB0001414	Putrescine	C4H12N2	88.1000
HMDB0000161	L-Alanine	C3H7NO2	89.0477
HMDB0000190	L-Lactic acid	C3H6O3	90.0317
HMDB0000131	Glycerol	C3H8O3	92.0473
HMDB0002142	Phosphoric acid	H3O4P	97.9769
HMDB0000060	Acetoacetic acid	C4H6O3	102.0317
HMDB0002176	Ethylmethylacetic acid	C5H10O2	102.0681
HMDB0003911	3-Aminoisobutanoic acid	C4H9NO2	103.0633
HMDB0000097	Choline	C5H13NO	103.0997
HMDB0000691	Malonic acid	C3H4O4	104.0110
HMDB0000357	3-Hydroxybutyric acid	C4H8O3	104.0473
HMDB0000187	L-Serine	C3H7NO3	105.0426
HMDB0000139	Glyceric acid	C3H6O4	106.0266
HMDB0000965	Hypotaurine	C2H7NO2S	109.0198
HMDB0061711	Methylphosphate	CH5O4P	111.9925
HMDB0000300	Uracil	C4H4N2O2	112.0273
HMDB0000828	N-Carbamoylaspartate	C5H8N2O	112.0637
HMDB0000562	Creatinine	C4H7N3O	113.0589
HMDB0000162	L-Proline	C5H9NO2	115.0633
HMDB0000134	Fumaric acid	C4H4O4	116.0110
HMDB0000532	Acetylglycine	C4H7NO3	117.0426
HMDB0000043	Betaine	C5H11NO2	117.0790
HMDB0000254	Succinic acid	C4H6O4	118.0266
HMDB0001863	2-Hydroxyvaleric acid	C5H10O3	118.0630
HMDB0001147	Aminomalonic acid	C3H5NO4	119.0219
HMDB0000167	L-Threonine	C4H9NO3	119.0582
HMDB0001368	3-Mercaptopyruvic acid	C3H4O3S	119.9881
HMDB0001366	Purine	C5H4N4	120.0436
HMDB0000574	L-Cysteine	C3H7NO2S	121.0198
HMDB0002127	3-Mercaptolactic acid	C3H6O3S	122.0038
HMDB0001870	Benzoic acid	C7H6O2	122.0368
HMDB0001406	Niacinamide	C6H6N2O	122.0480

HMDB ID	Name	Formula	Neutral mass (Da)
HMDB0002994	Erythritol	C4H10O4	122.0579
HMDB0001488	Nicotinic acid	C6H5NO2	123.0320
HMDB0000251	Taurine	C2H7NO3S	125.0147
HMDB0002329	Oxalic acid	C2H6O6	126.0164
HMDB0000262	Thymine	C5H6N2O2	126.0429
HMDB0000079	Dihydrothymine	C5H8N2O2	128.0586
HMDB0000267	pyroglutamic acid	C5H7NO3	129.0426
HMDB0000634	Citraconic acid	C5H6O4	130.0266
HMDB0000695	Ketoleucine	C6H10O3	130.0630
HMDB0000725	4-Hydroxyproline	C5H9NO3	131.0582
HMDB0000064	Creatine	C4H9N3O2	131.0695
HMDB0000687	L-Leucine	C6H13NO2	131.0946
HMDB0000661	Glutaric Acid	C5H8O4	132.0423
HMDB0000168	L-Asparagine	C4H8N2O3	132.0535
HMDB0001624	2-Hydroxyhexanoic acid	C6H12O3	132.0786
HMDB0000214	Ornithine	C5H12N2O2	132.0899
HMDB0000191	L-Aspartic acid	C4H7NO4	133.0375
HMDB0000156	L-Malic acid	C4H6O5	134.0215
HMDB0000742	Homocysteine	C4H9NO2S	135.0354
HMDB0000034	Adenine	C5H5N5	135.0545
HMDB0000613	Erythronic acid	C4H8O5	136.0372
HMDB0000157	Hypoxanthine	C5H4N4O	136.0385
HMDB0029806	Methyl nicotinate	C7H7NO2	137.0477
HMDB0001895	Salicylic acid	C7H6O3	138.0317
HMDB0000301	Urocanic acid	C6H6N2O2	138.0429
HMDB0001494	Acetylphosphate	C2H5O5P	139.9875
HMDB0002271	Imidazolepropionic acid	C6H8N2O2	140.0586
HMDB0000224	O-phosphoethanolamine	C2H8NO4P	141.0191
HMDB0004827	Proline betaine	C7H13NO2	143.0946
HMDB0041946	N-Nitrosoproline	C5H8N2O3	144.0535
HMDB0000482	Caprylic acid	C8H16O2	144.1150
HMDB0003464	4-Guanidinobutanoic acid	C5H11N3O2	145.0851
HMDB0000895	Acetylcholine	C7H15NO2	145.1103
HMDB0001257	Spermidine	C7H19N3	145.1579
HMDB0000208	Oxoglutaric acid	C5H6O5	146.0215
HMDB0000641	L-Glutamine	C5H10N2O3	146.0691
HMDB0000182	Lysine	C6H14N2O2	146.1055
HMDB0001161	4-Trimethylammoniobutanoic acid	C7H16NO2	146.1181
HMDB0000148	L-Glutamic acid	C5H9NO4	147.0532
HMDB0000606	D-2-Hydroxyglutaric acid	C5H8O5	148.0372
HMDB0000696	L-Methionine	C5H11NO2S	149.0511
HMDB0000956	Tartaric acid	C4H6O6	150.0164
HMDB0000283	Ribose	C5H10O5	150.0528
HMDB0000764	Hydrocinnamic acid	C9H10O2	150.0681
HMDB0000132	Guanine	C5H5N5O	151.0494
HMDB0000292	Xanthine	C5H4N4O2	152.0334

HMDB ID	Name	Formula	Neutral mass (Da)
HMDB0004194	N1-Methyl-4-pyridone-3-carboxamide	C7H8N2O2	152.0586
HMDB0002917	D-Xylitol	C5H12O5	152.0685
HMDB0000177	L-Histidine	C6H9N3O2	155.0695
HMDB0000816	Phosphoglycolic acid	C2H5O6P	155.9824
HMDB0000226	Orotic acid	C5H4N2O4	156.0171
HMDB0000462	Allantoin	C4H6N4O3	158.0440
HMDB0000847	Pelargonic acid	C9H18O2	158.1307
HMDB0012154	3-Dehydrocarnitine	C7H13NO3	159.0895
HMDB0000857	Pimelic acid	C7H12O4	160.0736
HMDB0028680	Alanine-alanine	C6H12N2O3	160.0848
HMDB0000510	Aminoadipic acid	C6H11NO4	161.0688
HMDB0000062	L-Carnitine	C7H15NO3	161.1052
HMDB0000355	3-Hydroxy-3-methylglutaric acid	C6H10O5	162.0528
HMDB0001890	Acetylcysteine	C5H9NO3S	163.0303
HMDB0003081	Fucose	C6H12O5	164.0685
HMDB0002005	Methionine sulfoxide	C5H11NO3S	165.0460
HMDB0000159	L-Phenylalanine	C9H11NO2	165.0790
HMDB0060256	L-Xylonate	C5H10O6	166.0477
HMDB0002199	Desaminotyrosine	C9H10O3	166.0630
HMDB0000263	Phosphoenolpyruvic acid	C3H5O6P	167.9824
HMDB0000289	Uric acid	C5H4N4O3	168.0283
HMDB0059778	2-Pyrroloylglycine	C7H8N2O3	168.0535
HMDB0001431	Pyridoxamine	C8H12N2O2	168.0899
HMDB0012247	L-2,3-Dihydrodipicolinate	C7H7NO4	169.0375
HMDB0002075	Pyridoxine	C8H11NO3	169.0739
HMDB0001473	Dihydroxyacetone phosphate	C3H7O6P	169.9980
HMDB0000126	Glycerol 3-phosphate	C3H9O6P	172.0137
HMDB0000721	Glycylproline	C7H12N2O3	172.0848
HMDB0000511	Capric acid	C10H20O2	172.1463
HMDB0011756	N-Acetyl-Leucine	C8H15NO3	173.1052
HMDB0000072	cis-Aconitic acid	C6H6O6	174.0164
HMDB0003070	Shikimic acid	C7H10O5	174.0528
HMDB0003357	N-Acetylornithine	C7H14N2O3	174.1004
HMDB0000517	L-Arginine	C6H14N4O2	174.1117
HMDB0000812	N-Acetyl-L-aspartic acid	C6H9NO5	175.0481
HMDB0003157	Guanidinosuccinic acid	C5H9N3O4	175.0593
HMDB0000904	Citrulline	C6H13N3O3	175.0957
HMDB0000259	Serotonin	C10H12N2O	176.0950
HMDB0000250	Pyrophosphate	H4O7P2	177.9432
HMDB0000078	Cysteinylglycine	C5H10N2O3S	178.0412
HMDB0003466	L-Gulonolactone	C6H10O6	178.0477
HMDB0029415	S-Carboxymethyl-L-cysteine	C5H9NO4S	179.0252
HMDB0000714	Hippuric acid	C9H9NO3	179.0582
HMDB0003269	Nicotinuric acid	C8H8N2O3	180.0535
HMDB0000122	D-Glucose	C6H12O6	180.0634
HMDB0000158	L-Tyrosine	C9H11NO3	181.0739

HMDB ID	Name	Formula	Neutral mass (Da)
HMDB0000755	Hydroxyphenyllactic acid	C9H10O4	182.0579
HMDB0000247	Sorbitol	C6H14O6	182.0790
HMDB0001565	Phosphocholine	C5H14NO4P	183.0660
HMDB0030097	5-Hydroxyisourate	C5H4N4O4	184.0233
HMDB0000272	O-Phosphoserine	C3H8NO6P	185.0089
HMDB0000807	3-Phosphoglyceric acid	C3H7O7P	185.9929
HMDB0000947	Undecanoic acid	C11H22O2	186.1620
HMDB0011626	Dodecanol	C12H26O	186.1984
HMDB0001276	N-Acetylspermidine	C9H21N3O	187.1685
HMDB0006029	N-Acetylglutamine	C7H12N2O4	188.0797
HMDB0000446	N-alpha-acetyllysine	C8H16N2O3	188.1161
HMDB0001138	N-Acetylglutamic acid	C7H11NO5	189.0637
HMDB0000679	Homocitrulline	C7H15N3O3	189.1113
HMDB0015673	N-Carbamylglutamate	C6H10N2O5	190.0590
HMDB0004095	5-Methoxytryptamine	C11H14N2O	190.1106
HMDB0011745	N-Acetyl-L-methionine	C7H13NO3S	191.0616
HMDB0000094	Citric acid	C6H8O7	192.0270
HMDB0000821	Phenylacetylglycine	C10H11NO3	193.0739
HMDB0003402	Lyxose	C6H10O7	194.0427
HMDB0000625	Gluconic acid	C6H12O7	196.0583
HMDB0032055	N-Acetylhistidine	C8H11N3O3	197.0800
HMDB0029422	L-Histidine trimethylbetaine	C9H15N3O2	197.1164
HMDB0000638	Dodecanoic acid	C12H24O2	200.1776
HMDB0028691	Alanyl-Leucine	C9H18N2O3	202.1317
HMDB0001256	Spermine	C10H26N4	202.2157
HMDB0000201	L-Acetylcarnitine	C9H17NO4	203.1158
HMDB0000929	L-Tryptophan	C11H12N2O2	204.0899
HMDB0000671	Indole-3-lactate	C11H11NO3	205.0739
HMDB0000512	N-Acetyl-L-phenylalanine	C11H13NO3	207.0895
HMDB0000684	L-Kynurenine	C10H12N2O3	208.0848
HMDB0001511	Phosphocreatine	C4H10N3O5P	211.0358
HMDB0012250	L-Aspartyl-4-phosphate	C4H8NO7P	213.0038
HMDB0000114	Glycerylphosphorylethanolamine	C5H14NO6P	215.0559
HMDB0004620	N-Acetyl-Arginine	C8H16N4O3	216.1222
HMDB0000856	N-a-Acetylcitrulline	C8H15N3O4	217.1063
HMDB0000824	Propionylcarnitine	C10H19NO4	217.1314
HMDB0000210	Pantothenic acid	C9H17NO5	219.1107
HMDB0000853	N-Acetyl-D-galactosamine	C8H15NO6	221.0899
HMDB0000099	L-Cystathionine	C7H14N2O4S	222.0674
HMDB0000866	N-Acetyl-L-tyrosine	C11H13NO4	223.0845
HMDB0002000	Myristoleic acid	C14H26O2	226.1933
HMDB0000014	Deoxycytidine	C9H13N3O4	227.0906
HMDB0000806	Myristic acid	C14H28O2	228.2089
HMDB0028739	Asparaginyl-proline	C9H15N3O4	229.1063
HMDB0001548	Ribose-5-phosphate	C5H11O8P	230.0192
HMDB0002013	Butyrylcarnitine	C11H21NO4	231.1471

HMDB ID	Name	Formula	Neutral mass (Da)
HMDB0000468	Biopterin	C9H11N5O3	237.0862
HMDB0012208	Erythro-imidazole-glycerol-phosphate	C6H11N2O6P	238.0355
HMDB0028853	Glycyl-tyrosine	C11H14N2O4	238.0954
HMDB0000192	L-Cystine	C6H12N2O4S2	240.0239
HMDB0000745	Homocarnosine	C10H16N4O3	240.1222
HMDB0000826	Pentadecanoic acid	C15H30O2	242.2246
HMDB0000089	Cytidine	C9H13N3O5	243.0855
HMDB0000296	Uridine	C9H12N2O6	244.0695
HMDB0028910	Ile-Ile	C12H24N2O3	244.1787
HMDB0013128	Valerylcarnitine	C12H23NO4	245.1627
HMDB0013713	N-acetyltryptophan	C13H14N2O3	246.1004
HMDB0011172	L-gamma-glutamyl-L-valine	C10H18N2O5	246.1216
HMDB0001491	Pyridoxal-5-phosphate	C8H10NO6P	247.0246
HMDB0029159	Gamma-glutamyl-Threonine	C9H17N3O5	247.1168
HMDB0001049	Gamma-glutamylcysteine	C8H14N2O5S	250.0623
HMDB0003229	Palmitoleic acid	C16H30O2	254.2246
HMDB0000220	Palmitic acid	C16H32O2	256.2402
HMDB0000086	Glycerophosphocholine	C8H20NO6P	257.1028
HMDB0012282	PPPi	H5O10P3	257.9096
HMDB0000884	Ribothymidine	C10H14N2O6	258.0852
HMDB0001401	Glucose 6-phosphate	C6H13O9P	260.0297
HMDB0011171	L-gamma-glutamyl-L-leucine	C11H20N2O5	260.1372
HMDB0000235	Thiamine	C12H17N4OS	265.1123
HMDB0001294	2,3-Diphosphoglyceric acid	C3H8O10P2	265.9593
HMDB0000050	Adenosine	C10H13N5O4	267.0968
HMDB0000195	Inosine	C10H12N4O5	268.0808
HMDB0060038	10Z-Heptadecenoic acid	C17H32O2	268.2402
HMDB0002259	Heptadecanoic acid	C17H34O2	270.2559
HMDB0002350	Octadecanol	C18H38O	270.2923
HMDB0001049	Gamma-Glutamyl-Glutamine	C10H17N3O6	275.1117
HMDB0001316	Phosphogluconic acid	C6H13O10P	276.0246
HMDB0004818	Biotin sulfone	C10H16N2O5S	276.0780
HMDB0011737	Gamma Glutamylglutamic acid	C10H16N2O7	276.0958
HMDB0000673	Linoleic acid	C18H32O2	280.2402
HMDB0002117	Oleamide	C18H35NO	281.2719
HMDB0002721	1-Methylinosine	C11H14N4O5	282.0964
HMDB0000207	Oleic acid	C18H34O2	282.2559
HMDB0000133	Guanosine	C10H13N5O5	283.0917
HMDB0001358	Retinal	C20H28O	284.2140
HMDB0000827	Stearic acid	C18H36O2	284.2715
HMDB0041876	Diacetylspermine	C14H30N4O2	286.2369
HMDB0005765	Ophthalmic acid	C11H19N3O6	289.1274
HMDB0001068	D-Sedoheptulose 7-phosphate	C7H15O10P	290.0403
HMDB0013622	Nonadeca-10(Z)-enoic acid	C19H36O2	296.2715
HMDB0000709	Cysteinylglycine disulfide	C8H15N3O5S2	297.0453
HMDB0001173	5'-Methylthioadenosine	C11H15N5O3S	297.0896

HMDB ID	Name	Formula	Neutral mass (Da)
HMDB0000772	Nonadecanoic acid	C19H38O2	298.2872
HMDB0000252	Sphingosine	C18H37NO2	299.2824
HMDB0001062	N-Acetylglucosamine phosphate	C8H15NO9S	301.0468
HMDB0001367	N-Acetyl-glucosamine 1-phosphate	C8H16NO9P	301.0563
HMDB0000269	Sphinganine	C18H39NO2	301.2981
HMDB0001067	N-Acetylaspartylglutamic acid	C11H16N2O8	304.0907
HMDB0001043	Arachidonic acid	C20H32O2	304.2402
HMDB0010378	5,8,11-Eicosatrienoic acid	C20H34O2	306.2559
HMDB0000125	GSH	C10H17N3O6S	307.0838
HMDB0061864	Dihomo-linoleate (20:2n6)	C20H36O2	308.2715
HMDB0000230	N-Acetylneuraminic acid	C11H19NO9	309.1060
HMDB0002231	Eicosenoic acid	C20H38O2	310.2872
HMDB0002212	Arachidic acid	C20H40O2	312.3028
HMDB0004610	Phytosphingosine	C18H39NO3	317.2930
HMDB0001227	5-Thymidylic acid	C10H15N2O8P	322.0566
HMDB0000095	Cytidine monophosphate	C9H14N3O8P	323.0519
HMDB0000288	Uridine 5'-monophosphate	C9H13N2O9P	324.0359
HMDB0002183	Docosahexaenoic acid	C22H32O2	328.2402
HMDB0000058	cAMP	C10H12N5O6P	329.0525
HMDB0001976	Docosapentaenoic acid (22n-6)	C22H34O2	330.2559
HMDB0011649	1-(sn-Glycero-3-phospho)-1D-myo-inositol	C9H19O11P	334.0665
HMDB0015186	Penicillin G	$C_{16}H_{18}N_2O_4S$	334.0987
HMDB0002823	Docosatrienoic acid	C22H38O2	334.2872
HMDB0000229	Nicotinamide D-ribonucleotide	C11H16N2O8P	335.0644
HMDB0061714	Docosadienoate (22:2n6)	C22H40O2	336.3028
HMDB0001058	Fructose 1,6-bisphosphate	C6H14O12P2	339.9961
HMDB0000186	Alpha-Lactose	C12H22O11	342.1162
HMDB0000045	AMP	C10H14N5O7P	347.0631
HMDB0000175	Inosine 5'-monophosphate (IMP)	C10H13N4O8P	348.0471
HMDB0000095	CMP	C11H15N2O9P	350.0515
HMDB00N/A	Phenol red	C19H14O5S	354.0562
HMDB0011567	MG(18:1(9Z)/0:0/0:0)	C21H40O4	356.2927
HMDB0001397	GMP	C10H14N5O8P	363.0580
HMDB0000939	S-Adenosylhomocysteine	C14H20N6O5S	384.1216
HMDB0000921	Cholestenone	C27H44O	384.3392
HMDB0000067	Cholesterol	C27H46O	386.3549
HMDB0000908	5alpha-Cholestanol	C27H48O	388.3705
HMDB0000280	Phosphoribosyl pyrophosphate	C5H13O14P3	389.9518
HMDB0001185	S-AdenosylMethionine	C15H22N6O5S	398.1372
HMDB0006119	7b-Hydroxycholesterol	C27H46O2	402.3498
HMDB0001546	CDP	C9H15N3O11P2	403.0182
HMDB0000295	UDP	C9H14N2O12P2	404.0022
HMDB0000256	Squalene	C30H50	410.3913
HMDB0041623	N6-Carbamoyl-L-threonyladenosine	C15H20N6O8	412.1343
HMDB0005065	Oleoylcarnitine	C25H47NO4	425.3505
HMDB0000656	Cysteineglutathione disulfide	C13H22N4O8S2	426.0879

HMDB ID	Name	Formula	Neutral mass (Da)
HMDB0001341	ADP	C10H15N5O10P2	427.0294
HMDB0001201	Guanosine diphosphate	C10H15N5O11P2	443.0243
HMDB0001564	CDP-ethanolamine	C11H20N4O11P2	446.0604
HMDB0011503	LysoPE(16:0/0:0)	C21H44NO7P	453.2855
HMDB0001520	Flavin Mononucleotide	C17H21N4O9P	456.1046
HMDB0000536	Adenylsuccinic acid	C14H18N5O11P	463.0740
HMDB0010379	LysoPC(14:0)	C22H46NO7P	467.3012
HMDB0011506	LysoPE(18:1(9Z)/0:0)	C23H46NO7P	479.3012
HMDB0011130	LysoPE(18:0/0:0)	C23H48NO7P	481.3168
HMDB0000082	Cytidine triphosphate	C9H16N3O14P3	482.9845
HMDB0000285	Uridine triphosphate	C9H15N2O15P3	483.9685
HMDB0001413	Citicoline	C14H26N4O11P2	488.1073
HMDB0011517	LysoPE(20:4(5Z,8Z,11Z,14Z)/0:0)	C25H44NO7P	501.2855
HMDB0000538	Adenosine triphosphate	C10H16N5O13P3	506.9958
HMDB0002815	LysoPC(18:1(9Z))	C26H52NO7P	521.3481
HMDB0001273	Guanosine triphosphate	C10H16N5O14P3	522.9907
HMDB0001178	Adenosine diphosphate ribose	C15H23N5O14P2	559.0717
HMDB0000935	Uridine diphosphate glucuronic acid	C15H22N2O18P2	580.0343
HMDB0001095	GDP-L-fucose	C16H25N5O15P2	589.0822
HMDB0000286	UDP-glucose	C15H24N2O17P2	566.0550
HMDB0000290	UDP-N-acetylglucosamine	C17H27N3O17P2	607.0816
HMDB0003337	Oxidized glutathione	C20H32N6O12S2	612.1520
HMDB0003502	Myo-inositol hexakisphosphate	C6H18O24P6	659.8614
HMDB0000902	NAD	C21H27N7O14P2	663.1091
HMDB0001487	NADH	C21H29N7O14P2	665.1248
HMDB0001296	Maltotetraose	C24H42O21	666.2219
HMDB0001373	Dephospho-CoA	C21H35N7O13P2S	687.1489
HMDB0001348	SM(d18:1/18:0)	C41H84N2O6P	731.6067
HMDB0000217	NADP	C21H28N7O17P3	743.0755
HMDB0000221	NADPH	C21H30N7O17P3	745.0911
HMDB0001423	Coenzyme A	C21H36N7O16P3S	767.1152
HMDB0001248	FAD	C27H33N9O15P2	785.1571
HMDB0001197	FADH	C27H35N9O15P2	787.1728
HMDB0001206	Acetyl-CoA	C23H38N7O17P3S	809.1258
HMDB0012254	Maltopentaose	C30H52O26	828.2747
HMDB0001022	Succinyl-CoA	C25H40N7O19P3S	867.1313

Table S-2. List of metabolites with reported concentrations of ≥ 1 μmol/mmol creatinine in the Urine Metabolome Database.[1]

HMDB ID	Name	Formula	Neutral mass (Da)
HMDB0000042	Acetic acid	C2H4O2	60.0211
HMDB0000294	Urea	CH4N2O	60.0324
HMDB0000149	Ethanolamine	C2H7NO	61.0528
HMDB0001525	Imidazole	C3H4N2	68.0374
HMDB0000474	Butanone	C4H8O	72.0575
HMDB0002134	Aminoacetone	C3H7NO	73.0528
HMDB0001522	Methylguanidine	C2H7N3	73.0640
HMDB0002501	Germanium	Ge	73.9212
HMDB0000119	Glyoxylic acid	C2H2O3	74.0004
HMDB0006961	Hydroxyacetone	C3H6O2	74.0368
HMDB0000123	Glycine	C2H5NO2	75.0320
HMDB0000925	Trimethylamine N-oxide	C3H9NO	75.0684
HMDB0000115	Glycolic acid	C2H4O3	76.0160
HMDB0001881	Propylene glycol	C3H8O2	76.0524
HMDB0002991	Cysteamine	C2H7NS	77.0299
HMDB0002500	Bromide	Br	78.9183
HMDB0001327	Rubidium	Rb	84.9118
HMDB0000243	Pyruvic acid	C3H4O3	88.0160
HMDB0001873	Isobutyric acid	C4H8O2	88.0524
HMDB0000161	L-Alanine	C3H7NO2	89.0477
HMDB0002329	Oxalic acid	C2H2O4	89.9953
HMDB0001311	D-Lactic acid	C3H6O3	90.0317
HMDB0000131	Glycerol	C3H8O3	92.0473
HMDB0003012	Aniline	C6H7N	93.0578
HMDB0004983	Dimethyl sulfone	C2H6O2S	94.0089
HMDB0000228	Phenol	C6H6O	94.0419
HMDB0001429	Phosphate	O4P	94.9534
HMDB0001448	Sulfate	O4S	95.9517
HMDB0002142	Phosphoric acid	H3O4P	97.9769
HMDB0000060	Acetoacetic acid	C4H6O3	102.0317
HMDB0000892	Valeric acid	C5H10O2	102.0681
HMDB0003911	3-Aminoisobutanoic acid	C4H9NO2	103.0633
HMDB0001352	Hydroxypyruvic acid	C3H4O4	104.0110
HMDB0000336	(R)-3-Hydroxyisobutyric acid	C4H8O3	104.0473
HMDB0002006	2,3-Diaminopropionic acid	C3H8N2O2	104.0586
HMDB0000097	Choline	C5H14NO	104.1075
HMDB0000187	L-Serine	C3H7NO3	105.0426
HMDB0006372	L-Glyceric acid	C3H6O4	106.0266
HMDB0033871	Benzylamine	C7H9N	107.0735
HMDB0001858	p-Cresol	C7H8O	108.0575
HMDB0000957	Pyrocatechol	C6H6O2	110.0368
HMDB0000630	Cytosine	C4H5N3O	111.0433

HMDB ID	Name	Formula	Neutral mass (Da)
HMDB0000257	Thiosulfate	O3S2	111.9289
HMDB0000617	2-Furoic acid	C5H4O3	112.0160
HMDB0000300	Uracil	C4H4N2O2	112.0273
HMDB0000562	Creatinine	C4H7N3O	113.0589
HMDB0003646	N-Methylhydantoin	C4H6N2O2	114.0429
HMDB0000134	Fumaric acid	C4H4O4	116.0110
HMDB0000720	Levulinic acid	C5H8O3	116.0473
HMDB0000128	Guanidoacetic acid	C3H7N3O2	117.0538
HMDB0000043	Betaine	C5H11NO2	117.0790
HMDB0000254	Succinic acid	C4H6O4	118.0266
HMDB0000754	3-Hydroxyisovaleric acid	C5H10O3	118.0630
HMDB0000719	L-Homoserine	C4H9NO3	119.0582
HMDB0000337	(S)-3,4-Dihydroxybutyric acid	C4H8O4	120.0423
HMDB0000574	L-Cysteine	C3H7NO2S	121.0198
HMDB0011718	4-Hydroxybenzaldehyde	C7H6O2	122.0368
HMDB0002994	Erythritol	C4H10O4	122.0579
HMDB0002243	Picolinic acid	C6H5NO2	123.0320
HMDB0000873	4-Methylcatechol	C7H8O2	124.0524
HMDB0000251	Taurine	C2H7NO3S	125.0147
HMDB0002024	Imidazoleacetic acid	C5H6N2O2	126.0429
HMDB0031306	3-Hydroxy-4,5-dimethyl-2(5H)-furanone	C6H8O3	128.0473
HMDB0000267	Pyroglutamic acid	C5H7NO3	129.0426
HMDB0000634	Citraconic acid	C5H6O4	130.0266
HMDB0000408	2-Methyl-3-ketovaleric acid	C6H10O3	130.0630
HMDB0002064	N-Acetylputrescine	C6H14N2O	130.1106
HMDB0000725	4-Hydroxyproline	C5H9NO3	131.0582
HMDB0000064	Creatine	C4H9N3O2	131.0695
HMDB0000687	L-Leucine	C6H13NO2	131.0946
HMDB0000223	Oxalacetic acid	C4H4O5	132.0059
HMDB0000661	Glutaric acid	C5H8O4	132.0423
HMDB0000168	L-Asparagine	C4H8N2O3	132.0535
HMDB0000317	2-Hydroxy-3-methylpentanoic acid	C6H12O3	132.0786
HMDB0006483	D-Aspartic acid	C4H7NO4	133.0375
HMDB0000156	L-Malic acid	C4H6O5	134.0215
HMDB0012141	(R)-2,3-Dihydroxy-isovalerate	C5H10O4	134.0579
HMDB0000742	Homocysteine	C4H9NO2S	135.0354
HMDB0000613	Erythronic acid	C4H8O5	136.0372
HMDB0000157	Hypoxanthine	C5H4N4O	136.0385
HMDB0002340	2-Methylbenzoic acid	C8H8O2	136.0524
HMDB0011659	2-Methylerythritol	C5H12O4	136.0736
HMDB0000875	Trigonelline	C7H7NO2	137.0477
HMDB0000699	1-Methylnicotinamide	C7H9N2O	137.0715
HMDB0001895	Salicylic acid	C7H6O3	138.0317
HMDB0013188	3-Hydroxypicolinic acid	C6H5NO3	139.0269
HMDB0004988	Pi-Methylimidazoleacetic acid	C6H8N2O2	140.0586
HMDB0000224	O-Phosphoethanolamine	C2H8NO4P	141.0191

HMDB ID	Name	Formula	Neutral mass (Da)
HMDB0002432	Sumiki's acid	C6H6O4	142.0266
HMDB0004827	Proline betaine	C7H13NO2	143.0946
HMDB0062511	octanoate radical	C8H15O2	143.1072
HMDB0000522	3-Methylglutaconic acid	C6H8O4	144.0423
HMDB0001988	4-Hydroxycyclohexylcarboxylic acid	C7H12O3	144.0786
HMDB0000730	Isobutyrylglycine	C6H11NO3	145.0739
HMDB0000208	Oxoglutaric acid	C5H6O5	146.0215
HMDB0000448	Adipic acid	C6H10O4	146.0579
HMDB0000641	L-Glutamine	C5H10N2O3	146.0691
HMDB0000182	L-Lysine	C6H14N2O2	146.1055
HMDB0003011	O-Acetylserine	C5H9NO4	147.0532
HMDB0059655	2-Hydroxyglutarate	C5H8O5	148.0372
HMDB0011600	3-Methyladenine	C6H7N5	149.0701
HMDB0001587	Phenylglyoxylic acid	C8H6O3	150.0317
HMDB0000098	D-Xylose	C5H10O5	150.0528
HMDB0011743	2-Phenylpropionate	C9H10O2	150.0681
HMDB0001878	Thymol	C10H14O	150.1045
HMDB0000403	2-Hydroxyadenine	C5H5N5O	151.0494
HMDB0001859	Acetaminophen	C8H9NO2	151.0633
HMDB0000786	Oxypurinol	C5H4N4O2	152.0334
HMDB0000020	p-Hydroxyphenylacetic acid	C8H8O3	152.0473
HMDB0004193	N1-Methyl-2-pyridone-5-carboxamide	C7H8N2O2	152.0586
HMDB0001851	L-Arabitol	C5H12O5	152.0685
HMDB0001476	3-Hydroxyanthranilic acid	C7H7NO3	153.0426
HMDB0000152	Gentisic acid	C7H6O4	154.0266
HMDB0000177	L-Histidine	C6H9N3O2	155.0695
HMDB0004812	2,5-Furandicarboxylic acid	C6H4O5	156.0059
HMDB0002320	Imidazolelactic acid	C6H8N2O3	156.0535
HMDB0000959	Tiglylglycine	C7H11NO3	157.0739
HMDB0000462	Allantoin	C4H6N4O3	158.0440
HMDB0000635	Succinylacetone	C7H10O4	158.0579
HMDB0000678	Isovalerylglycine	C7H13NO3	159.0895
HMDB0000857	Pimelic acid	C7H12O4	160.0736
HMDB0002467	A-Ketoglutaric acid oxime	C5H7NO5	161.0324
HMDB0002285	2-Indolecarboxylic acid	C9H7NO2	161.0477
HMDB0000510	Aminoadipic acid	C6H11NO4	161.0688
HMDB0000062	L-Carnitine	C7H15NO3	161.1052
HMDB0000640	Levoglucosan	C6H10O5	162.0528
HMDB0004350	Anabasine	C10H14N2	162.1157
HMDB0002169	S-(2-carboxypropyl)-Cysteamine	C6H13NO2S	163.0667
HMDB0000174	L-Fucose	C6H12O5	164.0685
HMDB0000159	L-Phenylalanine	C9H11NO2	165.0790
HMDB0002107	Phthalic acid	C8H6O4	166.0266
HMDB0001991	7-Methylxanthine	C6H6N4O2	166.0491
HMDB0000232	Quinolinic acid	C7H5NO4	167.0219
HMDB0240253	N-Acetyltaurine	C4H9NO4S	167.0252

HMDB ID	Name	Formula	Neutral mass (Da)
HMDB0000289	Uric acid	C5H4N4O3	168.0283
HMDB0000130	Homogentisic acid	C8H8O4	168.0423
HMDB0000439	2-Furoylglycine	C7H7NO4	169.0375
HMDB0000239	Pyridoxine	C8H11NO3	169.0739
HMDB0000479	3-Methylhistidine	C7H11N3O2	169.0851
HMDB0013312	trans-3-Octenedioic acid	C8H12O4	172.0736
HMDB0000511	Capric acid	C10H20O2	172.1463
HMDB0000701	Hexanoylglycine	C8H15NO3	173.1052
HMDB0000250	Pyrophosphate	O7P2	173.9119
HMDB0000072	cis-Aconitic acid	C6H6O6	174.0164
HMDB0000893	Suberic acid	C8H14O4	174.0892
HMDB0003357	N-Acetylornithine	C7H14N2O3	174.1004
HMDB0000517	L-Arginine	C6H14N4O2	174.1117
HMDB0000812	N-Acetyl-L-aspartic acid	C6H9NO5	175.0481
HMDB0003157	Guanidinosuccinic acid	C5H9N3O4	175.0593
HMDB0000197	Indoleacetic acid	C10H9NO2	175.0633
HMDB0000044	Ascorbic acid	C6H8O6	176.0321
HMDB0000714	Hippuric acid	C9H9NO3	179.0582
HMDB0001514	Glucosamine	C6H13NO5	179.0794
HMDB0000707	4-Hydroxyphenylpyruvic acid	C9H8O4	180.0423
HMDB0000660	D-Fructose	C6H12O6	180.0634
HMDB0001860	Paraxanthine	C7H8N4O2	180.0647
HMDB0011751	3-Methoxybenzenepropanoic acid	C10H12O3	180.0786
HMDB0013319	Tyrosinamide	C9H12N2O2	180.0899
HMDB0000158	L-Tyrosine	C9H11NO3	181.0739
HMDB0003099	1-Methyluric acid	C6H6N4O3	182.0440
HMDB0002643	3-(3-Hydroxyphenyl)-3-hydroxypropanoic acid	C9H10O4	182.0579
HMDB0000765	Mannitol	C6H14O6	182.0790
HMDB0001565	Phosphorylcholine	C5H15NO4P	184.0739
HMDB0000272	Phosphoserine	C3H8NO6P	185.0089
HMDB0011635	p-Cresol sulfate	C7H8O4S	188.0143
HMDB0006029	N-Acetylglutamine	C7H12N2O4	188.0797
HMDB0000784	Azelaic acid	C9H16O4	188.1049
HMDB0000206	N6-Acetyl-L-lysine	C8H16N2O3	188.1161
HMDB0002203	3-Hydroxycapric acid	C10H20O3	188.1412
HMDB0001325	N6,N6,N6-Trimethyl-L-lysine	C9H20N2O2	188.1525
HMDB0000715	Kynurenic acid	C10H7NO3	189.0426
HMDB0001138	N-Acetylglutamic acid	C7H11NO5	189.0637
HMDB0000325	3-Hydroxysuberic acid	C8H14O5	190.0841
HMDB0000763	5-Hydroxyindoleacetic acid	C10H9NO3	191.0582
HMDB0000094	Citric acid	C6H8O7	192.0270
HMDB0000821	Phenylacetylglycine	C10H11NO3	193.0739
HMDB0000127	D-Glucuronic acid	C6H10O7	194.0427
HMDB0001867	4-Aminohippuric acid	C9H10N2O3	194.0691
HMDB0006116	3-Hydroxyhippuric acid	C9H9NO4	195.0532
HMDB0000565	Galactonic acid	C6H12O7	196.0583

HMDB ID	Name	Formula	Neutral mass (Da)
HMDB0001857	1,3-Dimethyluric acid	C7H8N4O3	196.0596
HMDB0000291	Vanillylmandelic acid	C9H10O5	198.0528
HMDB0059771	6-amino-5[N-methylformylamino]-1-methyluracil	C7H10N4O3	198.0753
HMDB0013227	cis-5-Decenedioic acid	C10H16O4	200.1049
HMDB0000731	Cysteine-S-sulfate	C3H7NO5S2	200.9766
HMDB0000792	Sebacic acid	C10H18O4	202.1205
HMDB0001539	Asymmetric dimethylarginine	C8H18N4O2	202.1430
HMDB0000201	L-Acetylcarnitine	C9H17NO4	203.1158
HMDB0030396	(±)-Tryptophan	C11H12N2O2	204.0899
HMDB0000881	Xanthurenic acid	C10H7NO4	205.0375
HMDB0000379	2-Methylcitric acid	C7H10O7	206.0427
HMDB0001925	Ibuprofen	C13H18O2	206.1307
HMDB0000639	Galactaric acid	C6H10O8	210.0376
HMDB0001511	Phosphocreatine	C4H10N3O5P	211.0358
HMDB0000682	Indoxyl sulfate	C8H7NO4S	213.0096
HMDB0001885	3-Chlorotyrosine	C9H10ClNO3	215.0349
HMDB0004620	N-a-Acetyl-L-arginine	C8H16N4O3	216.1222
HMDB0000350	3-Hydroxysebacic acid	C10H18O5	218.1154
HMDB0000210	Pantothenic acid	C9H17NO5	219.1107
HMDB0000215	N-Acetyl-D-glucosamine	C8H15NO6	221.0899
HMDB0000099	L-Cystathionine	C7H14N2O4S	222.0674
HMDB0010325	Ethyl glucuronide	C8H14O7	222.0740
HMDB0000866	N-Acetyl-L-tyrosine	C11H13NO4	223.0845
HMDB0011631	L-3-Hydroxykynurenine	C10H12N2O4	224.0797
HMDB0011105	5-Acetylamino-6-formylamino-3-methyluracil	C8H10N4O4	226.0702
HMDB0000033	Carnosine	C9H14N4O3	226.1066
HMDB0000012	Deoxyuridine	C9H12N2O5	228.0746
HMDB0006695	Prolylhydroxyproline	C10H16N2O4	228.1110
HMDB0059911	Paracetamol sulfate	C8H9NO5S	231.0201
HMDB0002013	Butyrylcarnitine	C11H21NO4	231.1471
HMDB0000192	L-Cystine	C6H12N2O4S2	240.0239
HMDB0000194	Anserine	C10H16N4O3	240.1222
HMDB0000273	Thymidine	C10H14N2O5	242.0903
HMDB0000767	Pseudouridine	C9H12N2O6	244.0695
HMDB0000688	Isovalerylcarnitine	C12H23NO4	245.1627
HMDB0000497	5,6-Dihydrouridine	C9H14N2O6	246.0852
HMDB0000413	3-Hydroxydodecanedioic acid	C12H22O5	246.1467
HMDB0003229	Palmitoleic acid	C16H30O2	254.2246
HMDB0000220	Palmitic acid	C16H32O2	256.2402
HMDB0000982	5-Methylcytidine	C10H15N3O5	257.1012
HMDB0013161	2-Hexenoylcarnitine	C13H23NO4	257.1627
HMDB0013132	Hydroxyvalerylcarnitine	C12H25NO5	263.1733
HMDB0002381	N-Acetylcystathionine	C9H16N2O5S	264.0780
HMDB0006344	Alpha-N-Phenylacetyl-L-glutamine	C13H16N2O4	264.1110
HMDB0000830	Neuraminic acid	C9H17NO8	267.0954
HMDB0000050	Adenosine	C10H13N5O4	267.0968

HMDB ID	Name	Formula	Neutral mass (Da)
HMDB0000429	17a-Estradiol	C18H24O2	272.1776
HMDB0003331	1-Methyladenosine	C11H15N5O4	281.1124
HMDB0002721	1-Methylinosine	C11H14N4O5	282.0964
HMDB0000207	Oleic acid	C18H34O2	282.2559
HMDB0002372	N-Phenylacetylphenylalanine	C17H17NO3	283.1208
HMDB0000827	Stearic acid	C18H36O2	284.2715
HMDB0002089	N-Ribosylhistidine	C11H17N3O6	287.1117
HMDB0000791	L-Octanoylcarnitine	C15H29NO4	287.2097
HMDB0000788	Orotidine	C10H12N2O8	288.0594
HMDB0000234	Testosterone	C19H28O2	288.2089
HMDB0004667	13S-hydroxyoctadecadienoic acid	C18H32O3	296.2351
HMDB0001563	1-Methylguanosine	C11H15N5O5	297.1073
HMDB0013288	Nonanoylcarnitine	C16H31NO4	301.2253
HMDB0001067	N-Acetylaspartylglutamic acid	C11H16N2O8	304.0907
HMDB0001043	Arachidonic acid	C20H32O2	304.2402
HMDB0000230	N-Acetylneuraminic acid	C11H19NO9	309.1060
HMDB0000651	Decanoylcarnitine	C17H33NO4	315.2410
HMDB0002708	Cyanidin	C15H11ClO6	322.0244
HMDB0000600	Galactosylhydroxylysine	C12H24N2O8	324.1533
HMDB0010316	Acetaminophen glucuronide	C14H17NO8	327.0954
HMDB0002183	Docosahexaenoic acid	C22H32O2	328.2402
HMDB0001976	Docosapentaenoic acid (22n-6)	C22H34O2	330.2559
HMDB0004026	21-Hydroxypregnenolone	C21H32O3	332.2351
HMDB0000229	Nicotinamide ribotide	C11H15N2O8P	334.0566
HMDB0000944	Behenic acid	C22H44O2	340.3341
HMDB0000186	Alpha-Lactose	C12H22O11	342.1162
HMDB0001032	Dehydroepiandrosterone sulfate	C19H28O5S	368.1657
HMDB0013330	3-Hydroxy-cis-5-tetradecenoylcarnitine	C21H39NO5	385.2828
HMDB0001993	7a-Hydroxy-cholestene-3-one	C27H44O2	400.3341
HMDB0012173	4Alpha-hydroxymethyl-5alpha-cholesta-8-en-3beta-ol	C28H48O2	416.3654
HMDB0001341	ADP	C10H15N5O10P2	427.0294
HMDB0000797	SAICAR	C13H19N4O12P	454.0737
HMDB0006766	Estriol-16-Glucuronide	C24H32O9	464.2046
HMDB0000585	Glucosylgalactosyl hydroxylysine	C18H34N2O13	486.2061
HMDB0010318	Pregnanediol-3-glucuronide	C27H44O8	496.3036
HMDB0000302	Uridine diphosphategalactose	C15H24N2O17P2	566.0550
HMDB0004161	D-Urobilin	C33H40N4O6	588.2948
HMDB0004159	L-Urobilin	C33H46N4O6	594.3417
HMDB0003502	Myo-inositol hexakisphosphate	C6H18O24P6	659.8614
HMDB0007899	PC(14:1(9Z)/14:0)	C36H70NO8P	675.4839
HMDB0011234	PC(P-16:0/P-18:1(11Z))	C42H82NO6P	727.5880
HMDB0008029	PC(16:1(9Z)/P-18:1(11Z))	C42H80NO7P	741.5672
HMDB0007996	PC(16:0/P-18:1(11Z))	C42H82NO7P	743.5829
HMDB0011267	PC(P-18:0/P-18:1(11Z))	C44H86NO6P	755.6193
HMDB0007912	PC(14:1(9Z)/20:1(11Z))	C42H80NO8P	757.5622
HMDB0007911	PC(14:1(9Z)/20:0)	C42H82NO8P	759.5778

HMDB ID	Name	Formula	Neutral mass (Da)
HMDB0008062	PC(18:0/P-18:1(11Z))	C44H86NO7P	771.6142
HMDB0007919	PC(14:1(9Z)/22:0)	C44H86NO8P	787.6091
HMDB0013432	PC(o-18:1(9Z)/20:4(8Z,11Z,14Z,17Z))	C46H84NO7P	793.5985
HMDB0008752	PC(22:6(4Z,7Z,10Z,13Z,16Z,19Z)/P-18:0)	C48H84NO7P	817.5985
HMDB0008057	PC(18:0/22:6(4Z,7Z,10Z,13Z,16Z,19Z))	C48H84NO8P	833.5935
HMDB0013455	PC(o-22:2(13Z,16Z)/22:2(13Z,16Z))	C52H98NO7P	879.7081

Table S-3. Optimal sample dilution factors based on number of assigned metabolites for NAPA- and MALDI-MS analysis of hepatocyte extracts and urine.

	NAPA (+)	NAPA (–)	DHB (+)	9-AA (–)
Hep. Extr.	1×	1×	30×	1×
Urine	3×	3×	30×	10×

Table S-4. Complete listing of metabolites assigned from NAPA- and MALDI-MS analysis of hepatocyte extracts and their detected ionic species. Positive ion species are annotated as follows: "H", $[M+H]^+$; "H_2O", $[M+H-H_2O]^+$; "Na", $[M+Na]^+$; "K", $[M+K]^+$; "NaK", $[M+Na+K-H]^+$; "Na_2", $[M+2Na-H]^+$; "K_2", $[M+2K-H]^+$. Negative ion species are annotated as follows: "H", $[M-H]^-$; "H_2O", $[M-H-H_2O]^-$; "Na", $[M-2H+Na]^-$; "K", $[M-2H+K]^-$.'X' denotes detection of a metabolite by the given method (NAPA- or MALDI-MS) in the given polarity. The 'Total' column indicates detection of a compound in at least one polarity by the given technique.

		NAPA			MALDI		
Compound name	**Neutral mass (Da)**	**(+)**	**(–)**	**Total**	**(+)**	**(–)**	**Total**
Phosphoric acid	97.9769	**K, K_2**		**x**	**NaK, K_2**		**x**
Creatinine	113.0589	**Na, K, NaK, K_2**		**x**	**H, Na, K**		**x**
Threonine	119.0582	**NaK, K_2**		**x**	**H**		**x**
Taurine	125.0147	**NaK, K_2**	**H**	**x**	**NaK, Na_2, K_2**	**H**	**x**
Dihydrothymine	128.0586	**NaK, K_2**	**H**	**x**	**H**		**x**
Pyroglutamic acid	129.0426	**NaK, K_2**	**H, Na**	**x**	**H**	**H**	**x**
4-Hydroxyproline	131.0582	**NaK, K_2**		**x**	**H**		**x**
Creatine	131.0695	**Na, K, NaK, Na_2, K_2**		**x**	**H, Na, K, K_2**		**x**
Leucine	131.0946	**NaK, K_2**	**H**	**x**	**H**		**x**
Adenine	135.0545	**H, Na, K, K_2**	**H**	**x**	**H, K**	**H**	**x**
O-phosphoethanolamine	141.0191	**Na, K, K_2**	**H**	**x**		**H**	**x**
N-Nitrosoproline	144.0535	**K_2**		**x**		**H**	**x**
Glutamine	146.0691	**K, NaK, Na_2, K_2**	**H, Na**	**x**	**H, Na, K, NaK, K_2**	**H**	**x**
Glutamic acid	147.0532	**NaK, K_2**	**H, Na**	**x**	**H, Na, K, NaK, Na_2, K_2**	**H**	**x**
Guanine	151.0494	**K, NaK, K_2**	**H, H_2O**	**x**	**H, K**		**x**
Histidine	155.0695	**Na, K, NaK, K_2**	**H, Na, K**	**x**	**H, Na, K, NaK, K_2**	**H**	**x**
Pimelic acid	160.0736	**K_2**	**K**	**x**	**NaK, K_2**		**x**
Methionine sulfoxide	165.046	**K_2**		**x**		**H**	**x**
Dihydroxyacetone phosphate	169.998	**K_2**		**x**	**K_2**	**H_2O**	**x**
Glycerol 3-phosphate	172.0137	**K_2**	**H, H_2O**	**x**	**Na, NaK, K_2**		**x**
Arginine	174.1117	**K, NaK, K_2**	**H**	**x**	**H, K**		**x**
Pyrophosphate	177.9432	**K, NaK, K_2**		**x**	**Na, K, NaK, Na_2, K_2**	**H, H_2O**	**x**
Cysteinylglycine	178.0412	**K_2**		**x**	**H**	**H**	**x**

		NAPA			MALDI		
Compound name	**Neutral mass (Da)**	**(+)**	**(–)**	**Total**	**(+)**	**(–)**	**Total**
S-Carboxymethyl-L-cysteine	179.0252	**K_2**	**H**	**x**		**H_2O**	**x**
Glucose	180.0634	**Na, K, K_2**		**x**	**Na, K**		**x**
Tyrosine	181.0739	**K, NaK, K_2**	**H, H_2O, Na, K**	**x**		**H**	**x**
O-Phosphoserine	185.0089	**NaK, Na_2, K_2**	**H**	**x**	**NaK**		**x**
N-Acetylspermidine	187.1685	**Na, K**		**x**	**H, K**		**x**
Tryptophan	204.0899	**NaK, K_2**	**H**	**x**	**K**		**x**
Glycerylphosphoryl-ethanolamine	215.0559	**K, NaK, K_2**	**H, H_2O**	**x**	**Na, K, NaK, Na_2, K_2**	**H**	**x**
N-a-Acetylcitrulline	217.1063	**K_2**		**x**		**Na, K**	**x**
Pantothenic acid	219.1107	**Na, K, NaK, K_2**	**H**	**x**	**Na, K**	**H**	**x**
Cystathionine	222.0674	**K_2**		**x**	**K**		**x**
Deoxycytidine	227.0906	**K_2**		**x**		**H**	**x**
Asparaginyl-proline	229.1063	**NaK, K_2**		**x**		**H, H_2O**	**x**
Glycerophosphocholine	257.1028	**K, K_2**		**x**	**H, H_2O, Na, K**		**x**
Glutathione (red.)	307.0838	**K_2**	**H, Na, K**	**x**	**H, Na, K, NaK, Na_2, K_2**	**H, H_2O, Na, K**	**x**
Cytidine monophosphate	323.0519	**Na, K**	**K**	**x**	**K_2**	**H**	**x**
Cyclic AMP	329.0525	**K**		**x**	**H, H_2O, K**	**H**	**x**
Glycerophosphoinositol	334.0665	**K_2**	**H, H_2O**	**x**	**NaK, Na_2, K_2**	**H**	**x**
Penicillin G	334.0987	**K, K_2**		**x**	**H, K**		**x**
Phenol red	354.0562	**K_2**	**H, Na, K**	**x**		**H**	**x**
S-Adenosylmethionine	398.1372	**NaK**		**x**	**H**		**x**
Glutathione (ox.)	612.152	**K_2**		**x**	**Na, K, NaK, K_2**	**H, Na, K**	**x**
N-Acetylaspartic acid	175.0481		**H**	**x**	**K_2**	**H**	**x**
PPPi	257.9096		**Na**	**x**	**K, NaK, K_2**	**H, H_2O**	**x**
Glucose phosphate	260.0297		**H_2O**	**x**	**K, NaK, Na_2, K_2**	**H, H_2O**	**x**
Adenosine	267.0968		**K**	**x**	**H, H_2O, K, NaK, K_2**		**x**
Malondialdehyde	72.0211	**K_2**		**x**			
Glycine	75.032	**NaK, K_2**		**x**			
Cysteamine	77.0299	**NaK, K_2**		**x**			

		NAPA			MALDI		
Compound name	**Neutral mass (Da)**	**(+)**	**(–)**	**Total**	**(+)**	**(–)**	**Total**
Pyruvic acid	88.016	**NaK, K_2**		**x**			
Alanine	89.0477	**NaK, Na_2, K_2**		**x**			
Lactic acid	90.0317	**NaK, K_2**		**x**			
Serine	105.0426	**NaK, K_2**		**x**			
Methylphosphate	111.9925	**K, K_2**		**x**			
Uracil	112.0273	**K_2**		**x**			
Proline	115.0633	**NaK, Na_2, K_2**		**x**			
Acetylglycine	117.0426	**K_2**		**x**			
Betaine	117.079	**K, NaK, K_2**		**x**			
Succinic acid	118.0266	**K_2**		**x**			
Benzoic acid	122.0368	**K_2**		**x**			
Thymine	126.0429	**NaK, K_2**	**H, Na**	**x**			
Ornithine	132.0899	**H_2O, NaK, K_2**		**x**			
Homocysteine	135.0354	**K_2**		**x**			
Imidazolepropionic acid	140.0586	**K_2**		**x**			
Proline betaine	143.0946	**K_2**		**x**			
Lysine	146.1055	**NaK, K_2**	**H**	**x**			
Methionine	149.0511	**K_2**		**x**			
Phosphoglycolic acid	155.9824	**K_2**		**x**			
Pelargonic acid	158.1307	**K_2**		**x**			
3-Dehydrocarnitine	159.0895	**K_2**		**x**			
Alanine-alanine	160.0848	**K_2**		**x**			
Aminoadipic acid	161.0688	**K_2**		**x**			
Acetylcysteine	163.0303	**K_2**	**H_2O**	**x**			
Desaminotyrosine	166.063	**Na**		**x**			
Pyridoxamine	168.0899	**K_2**		**x**			
Glycylproline	172.0848	**NaK, K_2**	**H, H_2O, Na, K**	**x**			
Capric acid	172.1463	**K_2**		**x**			

		NAPA			MALDI		
Compound name	**Neutral mass (Da)**	**(+)**	**(–)**	**Total**	**(+)**	**(–)**	**Total**
N-Acetylornithine	174.1004	**H_2O, K_2**		**x**			
Undecanoic acid	186.162	**K_2**		**x**			
N-Acetylglutamine	188.0797	**K_2**		**x**			
N-Acetylglutamic acid	189.0637	K_2	**H**	**x**			
N-Acetylhistidine	197.08	**K_2**		**x**			
Dodecanoic acid	200.1776	**K_2**		**x**			
Aspartyl-4-phosphate	213.0038	**K_2**		**x**			
Myristic acid	228.2089	**K_2**		**x**			
Erythro-imidazole-glyc-erol-phosphate	238.0355	**Na_2**		**x**			
Pentadecanoic acid	242.2246	**K_2**		**x**			
Palmitoleic acid	254.2246	**K_2**		**x**			
Palmitic acid	256.2402	**NaK, K_2**		**x**			
Heptadecanoic acid	270.2559	**K_2**		**x**			
Biotin sulfone	276.078	**K, Na_2**		**x**			
Gamma-Glutamylglu-tamic acid	276.0958	**Na_2, K_2**		**x**			
Oleic acid	282.2559	**K_2**	**H**	**x**			
Stearic acid	284.2715	**K_2**		**x**			
N-Acetylaspartylglu-tamic acid	304.0907	**Na_2**		**x**			
Arachidonic acid	304.2402	**Na**		**x**			
5-Thymidylic acid	322.0566	**H**		**x**			
Lactose	342.1162	**K**		**x**			
3-Mercaptopyruvic acid	119.9881		**K**	**x**			
Purine	120.0436		**H**	**x**			
3-Mercaptolactic acid	122.0038		**K**	**x**			
Nicotinic acid	123.032		**H**	**x**			
Asparagine	132.0535		**Na**	**x**			
Hypoxanthine	136.0385		**H_2O**	**x**			
Methyl nicotinate	137.0477		**H_2O**	**x**			

		NAPA			MALDI		
Compound name	**Neutral mass (Da)**	**(+)**	**(–)**	**Total**	**(+)**	**(–)**	**Total**
Xanthine	152.0334		**H_2O**	**x**			
Phenylalanine	165.079		**H**	**x**			
Pyridoxine	169.0739		**H_2O**	**x**			
Hippuric acid	179.0582		**H_2O**	**x**			
Hydroxyphenyllactic acid	182.0579		**H_2O**	**x**			
Phenylacetylglycine	193.0739		**H_2O**	**x**			
Biopterin	237.0862		**K**	**x**			
Ribothymidine	258.0852		**H_2O**	**x**			
IMP	348.0471		**H_2O**	**x**			
Niacinamide	122.048				**H**		**x**
Citraconic acid	130.0266					**H_2O**	**x**
Aspartic acid	133.0375					**H**	**x**
Malic acid	134.0215					**H**	**x**
Salicylic acid	138.0317					**K**	**x**
Acetylcholine	145.1103				**H**		**x**
Spermidine	145.1579				**H**		**x**
Oxoglutaric acid	146.0215				**K_2**	**H**	**x**
Carnitine	161.1052				**H, Na, K**		**x**
Uric acid	168.0283					**H**	**x**
Aconitic acid	174.0164					**K**	**x**
Shikimic acid	174.0528				**K_2**	**K**	**x**
Nicotinuric acid	180.0535					**H**	**x**
Phosphocholine	183.066				**H, H_2O, Na, K**		**x**
N-alpha-acetyllysine	188.1161				**Na_2**		**x**
Citric acid	192.027				**NaK, K_2**	**H**	**x**
Acetylcarnitine	203.1158				**H**		**x**
Kynurenine	208.0848				**H**		**x**
Phosphocreatine	211.0358				**H, K**		**x**

		NAPA			MALDI		
Compound name	**Neutral mass (Da)**	**(+)**	**(–)**	**Total**	**(+)**	**(–)**	**Total**
Propionylcarnitine	217.1314				**H**		**x**
N-Acetylgalactosamine	221.0899				**H_2O**		**x**
Butyrylcarnitine	231.1471				**H, NaK**		**x**
Glycyl-tyrosine	238.0954				**H**		**x**
Cytidine	243.0855				**K_2**		**x**
Ile-Ile	244.1787				**K_2**		**x**
Valerylcarnitine	245.1627				**H**		**x**
Gamma-Glutamylleucine	260.1372				**K**		**x**
Gamma-Glutamylglutamine	275.1117				**K**		**x**
Guanosine	283.0917				**H, K, K_2**		**x**
Ophthalmic acid	289.1274				**K**		**x**
5'-Methylthioadenosine	297.0896				**H**		**x**
N-Acetylglucosamine phosphate	301.0563					**H, H_2O**	**x**
N-Acetylneuraminic acid	309.106				**K**		**x**
UMP	324.0359				**K_2**	**H, H_2O**	**x**
Fructose bisphosphate	339.9961				**H_2O**	**H, H_2O, K**	**x**
AMP	347.0631				**H, H_2O, Na, K, NaK, Na_2, K_2**	**H**	**x**
GMP	363.058				**K, NaK, K_2**	**H, K**	**x**
S-Adenosylhomocysteine	384.1216				**H**		**x**
Phosphoribosyl pyrophosphate	389.9518					**H_2O**	**x**
CDP	403.0182				**NaK, K_2**	**H, H_2O**	**x**
UDP	404.0022				**Na, K, NaK, Na_2, K_2**	**H, H_2O, Na, K**	**x**
ADP	427.0294				**H, H_2O, Na, K, NaK, Na_2, K_2**	**H, H_2O, Na, K**	**x**
GDP	443.0243				**H, K, K_2**	**H, H_2O, K**	**x**
Flavin Mononucleotide	456.1046				**H_2O, K**		**x**
CTP	482.9845				**K_2**	**H**	**x**
UTP	483.9685				**K_2**	**H, H_2O, Na, K**	**x**

		NAPA			MALDI		
Compound name	**Neutral mass (Da)**	**(+)**	**(–)**	**Total**	**(+)**	**(–)**	**Total**
ATP	506.9958				**H, K, NaK, K_2**	**H, H_2O, Na, K**	**x**
GTP	522.9907				**K, K_2**	**H, H_2O, K**	**x**
ADP-ribose	559.0717				**H, H_2O, K, K_2**	**H, H_2O**	**x**
UDP-glucuronic acid	580.0343					**H**	**x**
GDP-fucose	589.0822					**H**	**x**
UDP-glucose	597.0288				**K_2**	**H, Na, K**	**x**
UDP-N-acetylglucosamine	607.0816				**NaK, K_2**	**H, Na, K**	**x**
NAD	663.1091				**H, H_2O, Na, K, NaK, Na_2, K_2**		**x**
NADH	665.1248				**H, H_2O, Na, K, NaK, Na_2, K_2**	**H**	**x**
Dephospho-CoA	687.1489					**H**	**x**
NADP	743.0755				**H, K, NaK**		**x**
NADPH	745.0911				**H, K, NaK**	**H**	**x**
Coenzyme A	767.1152				**H, K, K_2**	**H, Na, K**	**x**
FAD	785.1571				**H, K, NaK, K_2**		**x**
FADH	787.1728					**H**	**x**
Maltopentaose	828.2747				**H_2O**		**x**

Table S-5. Complete listing of metabolites assigned from NAPA- and MALDI-MS analysis of urine and their detected ionic species. Positive ion species are annotated as follows: "H", $[M+H]^+$; "H_2O", $[M+H-H_2O]^+$; "Na", $[M+Na]^+$; "K", $[M+K]^+$; "NaK", $[M+Na+K-H]^+$; "Na_2", $[M+2Na-H]^+$; "K_2", $[M+2K-H]^+$. Negative ion species are annotated as follows: "H", $[M-H]^-$; "H_2O", $[M-H-H_2O]^-$; "Na", $[M-2H+Na]^-$; "K", $[M-2H+K]^-$ .. 'X' denotes detection of a metabolite by the given method (NAPA- or MALDI-MS) in the given polarity. The 'Total' column indicates detection of a compound in at least one polarity by the given technique.

		NAPA			MALDI		
Compound name	Neutral mass (Da)	(+)	(–)	Total	(+)	(–)	Total
Phosphoric acid	97.9769	K, NaK, Na_2, K_2		x	NaK, Na_2, K_2		x
Creatinine	113.0589	H, Na, K, NaK, Na_2, K_2	H	x	H, Na, K		x
Guanidoacetic acid	117.0538	Na, K, NaK, Na_2, K_2		x	H, Na		x
Taurine	125.0147	NaK, Na_2, K_2	H	x	NaK, Na_2, K_2	H	x
Creatine	131.0695	H_2O, Na, K, NaK, Na_2		x	H, H_2O, Na, K		x
Aspartic acid	133.0375	NaK, Na_2		x	Na_2		x
Trigonelline	137.0477	K	H, H_2O	x	H, Na, K		x
Pi-Methylimidazolea-cetic acid	140.0586	Na, NaK, K_2		x	H		x
Proline betaine	143.0946	Na, K		x	Na, K		x
Glutamine	146.0691	Na, K, NaK, Na_2, K_2	H, H_2O, Na	x	H, H_2O, Na, K, NaK, Na_2, K_2	H	x
O-Acetylserine	147.0532		H_2O	x	H_2O		x
3-Methyladenine	149.0701		H	x	H		x
Acetaminophen	151.0633	H_2O, Na, K, NaK, Na_2, K_2	H, H_2O, Na, K	x	H, Na, K, NaK, Na_2, K_2	H	x
N1-Methyl-2-pyri-done-5-carboxamide	152.0586	Na, K	H	x	H, Na, K		x
Histidine	155.0695	H, Na, NaK, Na_2, K_2	H, Na	x	H, Na		x
Tiglylglycine	157.0739	K_2	H_2O	x	H_2O		x
Carnitine	161.1052	H, H_2O		x	H, H_2O, Na, K		x
Uric acid	168.0283	H, H_2O, Na, K, NaK, Na_2, K_2	H, H_2O, Na, K	x		H, Na, K	x
3-Methylhistidine	169.0851	H, Na, K, NaK, Na_2, K_2	H	x	H, Na, K, NaK, Na_2		x
Indoleacetic acid	175.0633	Na, NaK, Na_2, K_2		x	Na		x

		NAPA			MALDI		
Compound name	**Neutral mass (Da)**	**(+)**	**(–)**	**To-tal**	**(+)**	**(–)**	**To-tal**
Hippuric acid	179.0582	**H, H_2O, Na, K, NaK, Na_2, K_2**	**H, H_2O, Na, K**	**x**		**H, K**	**x**
Mannitol	182.079	**Na, K, NaK**		**x**	**Na**		**x**
p-Cresol sulfate	188.0143	**NaK, Na_2, K_2**	**H, H_2O**	**x**	**NaK, Na_2, K_2**	**H**	**x**
N6,N6,N6-Trimethyl-lysine	188.1525	**H, K_2**		**x**	**H**		**x**
Citric acid	192.027	**NaK, K_2**	**H**	**x**	**Na, NaK, Na_2, K_2**	**H, H_2O**	**x**
Phenylacetylglycine	193.0739	**NaK, K_2**	**H_2O**	**x**	**H_2O**		**x**
Glucuronic acid	194.0427	**Na, NaK, Na_2, K_2**	**H, H_2O**	**x**		**H_2O**	**x**
4-Aminohippuric acid	194.0691	**NaK**	**K**	**x**		**K**	**x**
3-Hydroxyhippuric acid	195.0532	**Na, K, NaK, Na_2, K_2**	**H, Na**	**x**	**H, Na, NaK, Na_2**		**x**
6-amino-5[N-methyl-formylamino]-1-methyluracil	198.0753	**Na, K, NaK, Na_2, K_2**	**H**	**x**	**Na**	**H**	**x**
Asymmetric dime-thylarginine	202.143	**H, Na, K, NaK, Na_2**		**x**	**H, K**		**x**
Ibuprofen	206.1307	**Na, NaK, Na_2, K_2**		**x**	**Na**		**x**
Phosphocreatine	211.0358	**H_2O**		**x**	**H_2O**	**Na**	**x**
Indoxyl sulfate	213.0096	**NaK, K_2**		**x**	**NaK, Na_2, K_2**		**x**
3-Chlorotyrosine	215.0349		**H, Na, K**	**x**		**Na**	**x**
N-a-Acetylarginine	216.1222	**K, K_2**		**x**	**H**		**x**
Acetaminophen sul-fate	231.0201	**H, NaK, Na_2, K_2**	**H, H_2O, Na, K**	**x**	**NaK, Na_2, K_2**	**H, H_2O**	**x**
Anserine	240.1222	**Na, K, NaK, Na_2, K_2**	**H**	**x**	**H, Na, K**		**x**
Pseudouridine	244.0695	**Na, K, NaK, Na_2, K_2**	**H**	**x**	**Na**		**x**
5-Methylcytidine	257.1012	**K**		**x**	**H_2O**		**x**
N-Acetylcystathi-onine	264.078	**K, Na_2**		**x**	**Na_2**		**x**
Alpha-N-Phenyla-cetylglutamine	264.111	**Na, K, NaK, Na_2, K_2**	**H, H_2O, Na**	**x**	**H, H_2O, Na, K, NaK, Na_2, K_2**	**H**	**x**
1-Methyladenosine	281.1124	**Na**		**x**	**H, Na**		**x**
1-Methylinosine	282.0964	**H_2O, Na**	**Na**	**x**	**Na, K**	**K**	**x**
1-Methylguanosine	297.1073	**Na, K**		**x**	**Na, K**		**x**
Nonanoylcarnitine	301.2253	**H**		**x**	**H**		**x**
N-Acetylneuraminic acid	309.106	**NaK, K_2**	**H_2O, K**	**x**	**K, NaK, K_2**		**x**

		NAPA			MALDI		
Compound name	**Neutral mass (Da)**	**(+)**	**(–)**	**Total**	**(+)**	**(–)**	**Total**
Acetaminophen glucuronide	327.0954	**Na, K, NaK, Na_2, K_2**	**H, Na, K**	**x**	**Na, K, NaK, Na_2, K_2**	**H**	**x**
Lactose	342.1162	**Na, K**		**x**	**Na, K**		**x**
Aniline	93.0578				**Na, K**		**x**
Benzylamine	107.0735				**H**		**x**
2-Methyl-3-ketovaleric acid	130.063				**Na**		**x**
Arginine	174.1117				**H**		**x**
Kynurenic acid	189.0426				**H**		**x**
Acetylcarnitine	203.1158				**H**		**x**
Xanthurenic acid	205.0375				**H**		**x**
Butyrylcarnitine	231.1471				**H, K**		**x**
Hydroxyvaleryl-carnitine	263.1733				**H_2O**		**x**
Octanoylcarnitine	287.2097				**H, K**		**x**
Decanoylcarnitine	315.241				**H**		**x**
Dehydroepiandrosterone sulfate	368.1657					**H**	**x**
D-Urobilin	588.2948				**K**		**x**
2-Furoylglycine	169.0375	**Na, K, NaK, Na_2, K_2**	**H**	**x**			
1-Methyluric acid	182.044		**H**	**x**			
Glucosylgalactosyl hydroxylysine	486.2061	**Na, K, NaK, Na_2, K_2**	**H**	**x**			
Urea	60.0324	**K_2**		**x**			
Glyoxylic acid	74.0004	**NaK, K_2**		**x**			
Glycine	75.032	**Na, K, NaK, Na_2, K_2**		**x**			
Glycolic acid	76.016	**NaK, K_2**		**x**			
Cysteamine	77.0299	**K_2**		**x**			
Pyruvic acid	88.016	**NaK, Na_2, K_2**		**x**			
Alanine	89.0477	**NaK, Na_2, K_2**		**x**			
Acetoacetic acid	102.0317	**NaK, Na_2, K_2**		**x**			
3-Aminoisobutanoic acid	103.0633	**Na_2**		**x**			
3-Hydroxyisobutyric acid	104.0473	**NaK, Na_2, K_2**		**x**			

		NAPA			MALDI		
Compound name	**Neutral mass (Da)**	**(+)**	**(–)**	**To-tal**	**(+)**	**(–)**	**To-tal**
Serine	105.0426	**NaK, Na_2, K_2**		**x**			
Cytosine	111.0433	**NaK, K_2**		**x**			
2-Furoic acid	112.016	**K_2**	**H**	**x**			
Levulinic acid	116.0473	**NaK, Na_2, K_2**		**x**			
Betaine	117.079	**Na, K, NaK**		**x**			
Succinic acid	118.0266	**H, NaK, Na_2, K_2**		**x**			
3-Hydroxyisovaleric acid	118.063	**NaK, Na_2**		**x**			
Homoserine	119.0582	**NaK, Na_2, K_2**		**x**			
3,4-Dihydroxybutyric acid	120.0423	**NaK, Na_2, K_2**		**x**			
Erythritol	122.0579	**Na, NaK, K_2**		**x**			
Picolinic acid	123.032	**NaK, K_2**		**x**			
Pyroglutamic acid	129.0426	**NaK, Na_2, K_2**		**x**			
Citraconic acid	130.0266	**NaK, K_2**		**x**			
4-Hydroxyproline	131.0582	**Na, NaK, Na_2, K_2**		**x**			
Glutaric acid	132.0423	**NaK, Na_2, K_2**	**H_2O**	**x**			
Asparagine	132.0535	**Na, NaK, Na_2, K_2**		**x**			
2,3-Dihydroxy-isova-lerate	134.0579	**NaK, Na_2, K_2**	**H**	**x**			
Erythronic acid	136.0372	**NaK, Na_2, K_2**	**H**	**x**			
Hypoxanthine	136.0385		**H_2O**	**x**			
2-Methylerythritol	136.0736	**NaK, K_2**		**x**			
O-Phosphoethanola-mine	141.0191	**Na, K, NaK, K_2**	**Na**	**x**			
Sumiki's acid	142.0266	**NaK, Na_2, K_2**		**x**			
3-Methylglutaconic acid	144.0423		**H_2O**	**x**			
Isobutyrylglycine	145.0739	**Na, Na_2**	**H**	**x**			
Oxoglutaric acid	146.0215	**NaK**		**x**			
Adipic acid	146.0579	**Na, NaK, Na_2, K_2**		**x**			
Lysine	146.1055	**H, Na, NaK, Na_2, K_2**	**H**	**x**			
2-Hydroxyglutarate	148.0372	**K_2**	**H, H_2O**	**x**			

		NAPA			MALDI		
Compound name	**Neutral mass (Da)**	**(+)**	**(–)**	**To-tal**	**(+)**	**(–)**	**To-tal**
Xylose	150.0528	**Na, Na_2**	**H**	**x**			
Oxypurinol	152.0334	**K_2**	**H, H_2O**	**x**			
p-Hydroxyphenyla-cetic acid	152.0473	**K_2**	**H, K**	**x**			
Arabitol	152.0685	**Na, K_2**		**x**			
3-Hydroxyanthranilic acid	153.0426		**H_2O**	**x**			
2,5-Furandicarboxylic acid	156.0059		**H_2O**	**x**			
Imidazolelactic acid	156.0535		**H_2O**	**x**			
Succinylacetone	158.0579		**H**	**x**			
Isovalerylglycine	159.0895	**Na**		**x**			
2-Indolecarboxylic acid	161.0477	**Na, NaK, Na_2**		**x**			
Aminoadipic acid	161.0688	**Na, NaK, Na_2, K_2**	**H**	**x**			
Levoglucosan	162.0528	**Na, NaK, Na_2, K_2**	**H_2O**	**x**			
Fucose	164.0685	**Na**	**H_2O**	**x**			
Phenylalanine	165.079	**NaK, Na_2**	**H**	**x**			
Phthalic acid	166.0266	**NaK, Na_2**		**x**			
7-Methylxanthine	166.0491	**NaK, Na_2, K_2**	**H**	**x**			
N-Acetyltaurine	167.0252	**K_2**		**x**			
Homogentisic acid	168.0423	**K_2**	**H**	**x**			
Pyridoxine	169.0739	**K_2**		**x**			
Hexanoylglycine	173.1052	**NaK, K_2**		**x**			
Suberic acid	174.0892	**K, NaK, K_2**		**x**			
N-Acetylornithine	174.1004	**NaK, K_2**	**H_2O**	**x**			
N-Acetyl-L-aspartic acid	175.0481	**Na_2**	**H**	**x**			
Guanidinosuccinic acid	175.0593	**H**		**x**			
Ascorbic acid	176.0321	**Na, NaK, Na_2, K_2**	**H_2O**	**x**			
Fructose	180.0634	**Na, K**	**H_2O**	**x**			
Tyrosine	181.0739	**NaK, Na_2, K_2**	**H, H_2O**	**x**			
3-(3-Hydroxyphenyl)-3-hydroxypropanoic acid	182.0579	**NaK, K_2**	**H, H_2O**	**x**			

		NAPA			MALDI		
Compound name	**Neutral mass (Da)**	**(+)**	**(–)**	**To-tal**	**(+)**	**(–)**	**To-tal**
N-Acetylglutamine	188.0797	**Na, NaK, Na_2, K_2**	**H**	**x**			
N6-Acetyl-L-lysine	188.1161	**Na, Na_2**	**H**	**x**			
3-Hydroxycapric acid	188.1412		**K**	**x**			
3-Hydroxysuberic acid	190.0841	**K, K_2**		**x**			
5-Hydroxyindoleace-tic acid	191.0582	**Na, NaK, Na_2, K_2**		**x**			
Galactonic acid	196.0583		**H_2O**	**x**			
Sebacic acid	202.1205	**Na, NaK, K_2**		**x**			
Tryptophan	204.0899	**Na, NaK, Na_2, K_2**	**H**	**x**			
3-Hydroxysebacic acid	218.1154	**K_2**		**x**			
N-Acetylglucosamine	221.0899	**Na, K**		**x**			
Ethyl glucuronide	222.074	**Na, NaK, Na_2, K_2**	**H**	**x**			
5-Acetylamino-6-formylamino-3-methyluracil	226.0702	**NaK, Na_2, K_2**	**K**	**x**			
Carnosine	226.1066	**NaK, Na_2, K_2**		**x**			
Prolylhydroxyproline	228.111	**NaK, Na_2, K_2**		**x**			
3-Hydroxydodecane-dioic acid	246.1467	**K_2**		**x**			
Neuraminic acid	267.0954	**NaK, K_2**	**H_2O, K**	**x**			
Orotidine	288.0594	**H**		**x**			
Galactosylhydroxyly-sine	324.1533	**H, Na, K_2**		**x**			
L-Urobilin	594.3417	**H_2O**		**x**			

Table S-6. Ionic species distributions for assigned metabolite ions in positive ion mode NAPA- and MALDI-MS of hepatocyte extracts and urine at optimal dilution factor (see Table S-3). All values are % of total assigned metabolite signal.

		$[M+H]^+$	$[M+H-H_2O]^+$	$[M+Na]^+$	$[M+2Na-H]^+$	$[M+Na+K-H]^+$	$[M+K]^+$	$[M+2K-H]^+$
Hep. Extr.	*NAPA*	0.3	0.0	0.3	2.4	9.0	2.8	85.2
	MALDI	20.5	7.5	6.8	0.8	12.2	28.6	23.6
Urine	*NAPA*	0.5	0.1	14.0	12.5	30.7	13.5	28.6
	MALDI	18.6	15.4	30.7	6.8	5.3	18.8	4.4

Table S-7. Ionic species distributions for assigned metabolite ions in negative ion mode NAPA- and MALDI-MS of hepatocyte extracts and urine at optimal dilution factor (see Table S-3). All values are % of total assigned metabolite signal.

		$[M-H]^-$	$[M-H-H2O]^-$	$[M-2H+Na]^-$	$[M-2H+K]^-$
Hep. Extr.	*NAPA*	72.4	19.2	2.8	5.6
	MALDI	69.5	19.3	4.0	7.2
Urine	*NAPA*	88.3	4.4	6.7	0.6
	MALDI	76.1	5.1	16.9	2.0

REFERENCE

(1) Bouatra, S.; Aziat, F.; Mandal, R.; Guo, A. C.; Wilson, M. R.; Knox, C.; Bjorndahl, T. C.; Krishnamurthy, R.; Saleem, F.; Liu, P.; Dame, Z. T.; Poelzer, J.; Huynh, J.; Yallou, F. S.; Psychogios, N.; Dong, E.; Bogumil, R.; Roehring, C.; Wishart, D. S. *PLoS One* **2013**, *8*, e73076.